Adv Polym Sci (2016) 273: 59–112
DOI: 10.1007/12_2015_345

Published online: 17 December 2015

Intrinsic Self-Healing Polymers Based on Supramolecular Interactions: State of the Art and Future Directions

Marcel Enke, Diana Döhler, Stefan Bode, Wolfgang H. Binder, Martin D. Hager, and Ulrich S. Schubert

Abstract Supramolecular polymers are an intriguing class of materials with dynamic behavior as a result of the presence of non-covalent bonds. These bonds include hydrogen bonds, metallopolymers, ionomers, host–guest as well as π–π interactions. The strength of these supramolecular bonds can be tuned by varying the binding motifs. Their reversible and dynamic character can be utilized to engineer self-healing polymers. This review briefly presents the preconditions for design of self-healing polymers and summarizes the development of supramolecular self-healing polymers based on various non-covalent interactions. Furthermore, challenges and perspectives for the understanding of self-healing mechanisms and the preparation of novel materials with enhanced properties are discussed.

Keywords Host–guest interactions • Hydrogen bonding • Metallopolymers • Self-healing • Supramolecular polymers

---

Marcel Enke and Diana Döhler are equally contributed.

M. Enke, S. Bode, M.D. Hager (✉), and U.S. Schubert (✉)
Laboratory of Organic and Macromolecular Chemistry (IOMC), Friedrich Schiller University Jena, Humboldtstrasse 10, 07743 Jena, Germany

Jena Center for Soft Matter (JCSM), Friedrich Schiller University Jena, Philosophenweg 7, 07743 Jena, Germany
e-mail: martin.hager@uni-jena.de; ulrich.schubert@uni-jena.de

D. Döhler and W.H. Binder (✉)
Chair of Macromolecular Chemistry, Faculty of Natural Science II (Chemistry, Physics and Mathematics), Martin Luther University Halle-Wittenberg, Von-Danckelmann-Platz 4, 06120 Halle (Saale), Germany
e-mail: wolfgang.binder@chemie.uni-halle.de

Contents

1 Introduction

Inspired by nature – more precisely by the greater burdock – the Swiss electrical engineer de Mestral invented Velcro and enabled the reversible connection of two textile components. This function is based on the interconnection of many hooks with the corresponding loops, leading to an effective "binding." Supramolecular polymers feature a kind of molecular hook-and-loop fastener because of their reversible supramolecular interactions (e.g., hydrogen bonds, metal–ligand interactions, and host–guest interactions). These materials offer great opportunities for the design of smart materials (e.g., stimuli-responsive materials) [1–4] or even self-healing materials, as a result of their non-covalent secondary interactions within the polymeric structure [5, 6].

All those interactions feature a dynamic character, which is essential in the design of self-healing materials [7, 8]. The self-healing mechanism of supramolecular polymers is based on the re-association of non-covalent interactions and clusters, or on the stimuli-responsive opening and closing of the supramolecular binding unit, depending on the binding strength of the utilized interaction (Fig. 1).

To achieve a healing response, a sufficient level of chain dynamics is required to enable mobility of the supramolecular motifs within the bulk material [9], which is related to the time required to renew the chain conformation under unstrained conditions and to reestablish the equilibrium [10, 11]. Thus, motion of the whole polymer chain is controlled by the lifetime and concentration of supramolecular tie points. However, the polymer chains can also diffuse at timescales longer than the lifetime of the supramolecular interactions [12, 13].

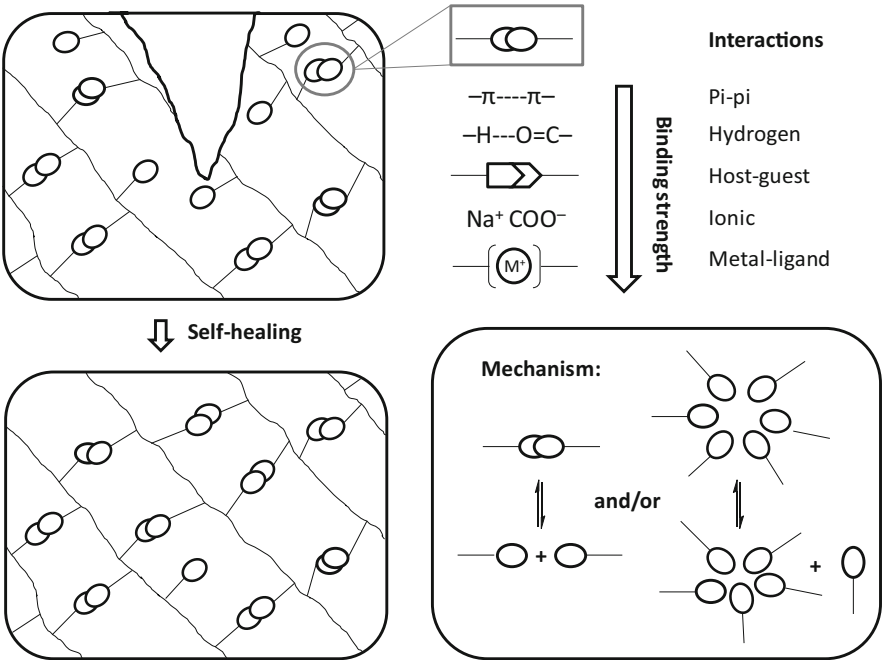

Fig. 1 *Left*: Scheme of the self-healing process. *Top right*: Supramolecular interactions ordered by their binding strength. *Bottom right*: Proposed self-healing mechanism of supramolecular polymers based on either cluster formation and/or stimuli-responsive opening of the non-covalent binding unit

Strong supramolecular interactions are associated with a high binding constant and are comparable to covalent bonds. In analogy to dynamic covalent bonds (e.g., Diels–Alder units) [14–16], the self-healing mechanism is not solely based on the presence of residual supramolecular binding after mechanical damage.

The first accidental approach towards self-healing of supramolecular polymers is already over 25 years old [17–20] and relies on the use of weak stickers (urazole moieties) affixed onto butadiene polymers, leading to reversible, sticky moieties within a thermoplastic material. Without being intentional, such supramolecular polymers display intrinsic self-healing properties, as demonstrated by their viscoelastic properties [18] and the resulting chain dynamics – an idea taken up later in the intentional design of rubbers with self-healing properties [21]. A second (old) concept is based on ionic clusters embedded in the polymeric matrix to achieve dynamic properties via ionic clusters formed according to the Eisenberg–Moore–Hird model [22], resulting in self-healing ionomers. In a similar manner, ureidopyrimidone (UPy) units affixed onto terminal functionalized monomers and bound by strong self-dimerization with four cooperative hydrogen bonds, lead to significant improvement in material properties as a result of the additional non-covalent crosslinks and, thus, can introduce dynamic properties into a thermoplastic material [23].

This chapter presents different supramolecular polymer classes, set apart by the nature of their non-covalent interactions, that have been used for the design of self-

healing materials. We focus on the following supramolecular interactions: Hydrogen bonds, π–π interactions, ionic interactions, metal–ligand interactions, and host–guest recognition. In this context, the state of the art for each class of polymers is summarized in detail.

2 Hydrogen-Bonded Supramolecular Self-Healing

2.1 Hydrogen Bonding Interactions and Their Principal Role in Self-Healing Polymers

Supramolecular self-healing concepts offer the possibility to create self-healing materials that can heal local damage multiple times. Hydrogen bonding interactions in particular play a key role because of their highly dynamic nature and responsiveness to external stimuli, in combination with a tunable and directed association strength [24]. Accordingly, supramolecular polymers with incorporated hydrogen bonding moieties are at the front line for industrial applications. A selection of different hydrogen bonding moieties used to induce self-healing are highlighted in Fig. 2.

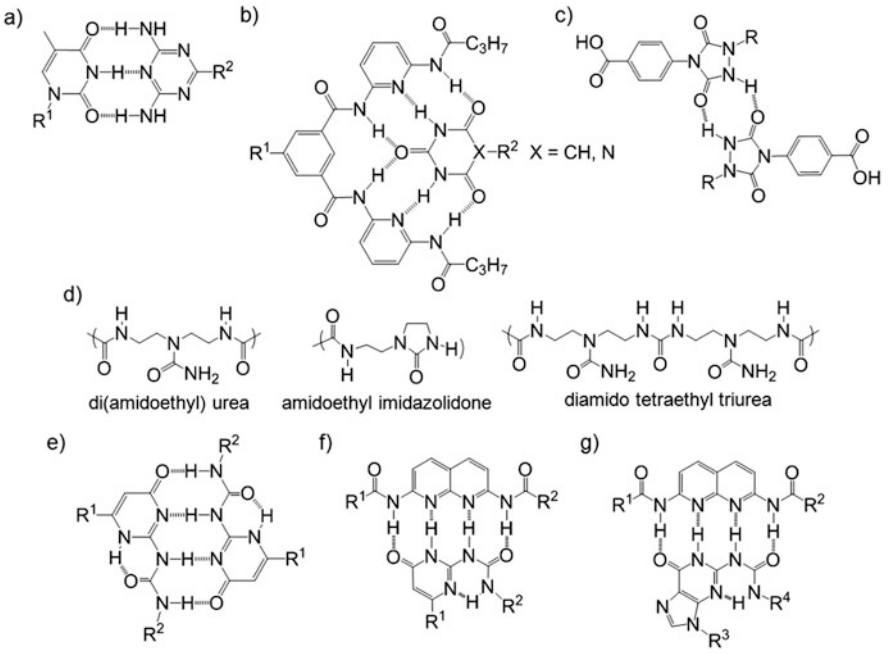

Fig. 2 Hydrogen bonding moieties useful for incorporating of self-healing properties into polymers: (**a**) Thymine (THY) and diaminotriazine (DAT), (**b**) Hamilton wedge and cyanuric/barbituric acid wedge, (**c**) two phenyl urazole acids, (**d**) components forming a self-healing rubber, (**e**) ureidopyrimidones (UPy), (**f**) UPy and 2,7-diamido-1,8-naphthyridine (DAN), and (**g**) DAN and ureido-7-deazaguanine (DeUG)

Thus, a large structural variety of hydrogen bonding moieties exists, which allows tuning of the stability/lability and, therefore, of the inherent dynamics of hydrogen-bonded polymers. However, self-healing is not only determined by the absolute strength of the applied hydrogen bonds [25], but also by phase segregation effects between the polymeric interphases [26, 27]. The strength of hydrogen bonds in the solid and melt states of polymers is generally not known and is certainly different from the values known from polymer solutions. Even "weak" bonds in solution can exert a significant effect on self-healing, whereas "strong" bonds often display no or retarded self-healing effects. Thus, nanophase separation between hard and soft domains within a copolymer or composite material, or the crystallization or clustering of introduced supramolecular moieties, can introduce a self-healing response based on the autonomous rearrangement between hard and soft phases after a damage event.

A representative example of these effects can be seen by comparing association constants within the well-investigated THY–DAT trivalent hydrogen bonding system (Fig. 2a). The possible modes of aggregation for the supramolecular groups A (DAT) and B (THY) in solution and in the melt are schematically illustrated in Fig. 3.

In solution, the THY–DAT interaction is usually stronger than the self-association of each building unit with itself (i.e. dimerization), resulting in specific a interaction according to the lock-and-key model [$K_{\mathrm{dim1}} \approx K_{\mathrm{dim2}} \ll K_{\mathrm{assn.}}$, K_{dim1}

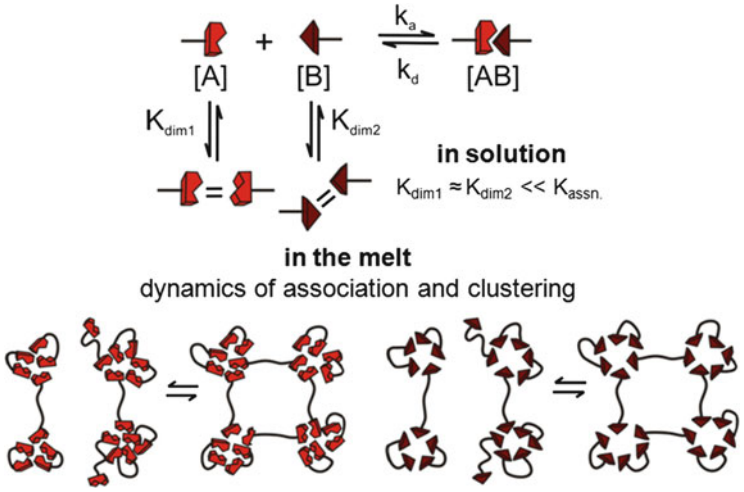

Fig. 3 Possible modes of aggregation for supramolecular groups *A* and *B* in solution and in the melt. Figure reprinted and adopted from [28] with permission from The Royal Society of Chemistry (Copyright 2012)

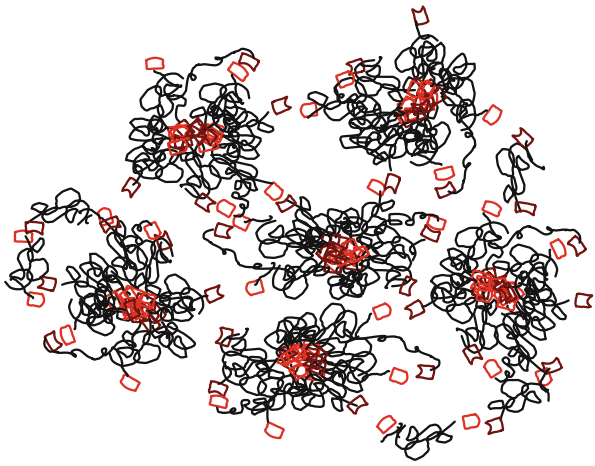

Fig. 4 Crosslinked supramolecular micelles composed of bivalent THY- and DAT-telechelic PIBs. Figure reprinted and adopted with permission from [26] (Copyright (2014) American Chemical Society)

(THY–THY) = 70 ± 14 M^{-1}, K_{dim2} (DAT–DAT) = 22 ± 7 M^{-1}, $K_{assn.}$ (THY–DAT) = 2.6 ± 1.3 × 10^3 M^{-1}]. In contrast, in the molten state (e.g., the same polymer system without any solvent) the dynamics of association and, therefore, the clustering of complementary hydrogen bonding units, often overrides a simple AB interaction, resulting in self-aggregation of DAT–DAT units or THY–THY units comparable to that of the THY–DAT system in solution [25].

Thus, combined and detailed rheology and small-angle X-ray scattering (SAXS) investigations of polymer blends composed of bivalent THY- and DAT-telechelic poly(isobutylene)s (PIBs) revealed the formation of a supramolecular network of supramolecular crosslinked disordered micelles (Fig. 4). The formation of linear supramolecular chains followed by entanglement or the presence of ordered micellar structures could be clearly excluded [26].

Inspired by the design of self-healing polymers with exchangeable and therefore weak covalent bonds [29, 30], hybrid computational models [31–33] have been applied to predict the influence of the fraction of permanent and labile bonds, in turn simulating the mechanism of strain recovery. Thus, a competitive effect between the extent and the rate of strain recovery was proven via calculations. For an increasing labile bond energy, related to the increased time scale required for strain recovery, a tougher material with improved mechanical properties was obtained. In contrast, an increasing amount of permanent bonds provided better and faster strain recovery after exposure to several stretch–relaxation cycles. The incorporation of a small fraction of labile bonds (20–30%) resulted in a significant improvement in tensile strength, while at the same time creating an additional self-healing response after tensile deformation. Thus, labile bonds acted as sacrificial species while dissipating the energy emerging from a rupture event by structural rearrangements and preserving the overall mechanical integrity [30, 34].

2.2 Fatty Acid-Based Formation of Thermoplastic Elastomers

Thermoreversible supramolecular polymers with a low glass transition temperature (T_g) have been formed by hydrogen bonding interactions between polyamide oligomers prepared from fatty diacids treated with sulfonyl isocyanate and ethylenediamine [35]. The obtained thermoplastic elastomers (s) exhibited a high rubbery plateau and the introduced rubber elasticity resulted in 88% recovery of the tensile strength after keeping reassembled samples at 50 °C for 18 h [35].

In a very similar manner, poly(dimethyl siloxane) (PDMS)-based supramolecular elastomers associated via multiple hydrogen bonding interactions and therefore showing a low temperature self-healing response have been prepared. The rubber-like elastic behavior allowed imposed formations to recover within seconds after releasing the stress [36]. The preparation of a soft supramolecular rubber [37–40] by condensing diethylene triamine and urea with a mixture of multiply functionalized fatty acids (Fig. 2d) has also been reported. The degree of branching was controlled by the choice of fatty acids and by adjusting their ratio. Thus, complementary hydrogen bonding units were incorporated in the resulting oligomeric material, plasticized with dodecane (11 wt%) to lower its (T_g) to 8 °C. Complete self-healing of cut pieces was observed within 3 h at room temperature. The maximum waiting time for keeping cut samples apart from each other before allowing self-healing was 48 h at 48 °C [37], but healing was completely suppressed by annealing at 90 °C as a result of equilibrating hydrogen bonding moieties [41]. Consequently, the required healing time related to the re-association of hydrogen bonding interactions strongly depends on the mobility of the whole polymer backbone, as reorganization over a larger length scale within the bulk material is required [41]. Furthermore, the strength required to separate a formerly cracked and subsequently healed surface was significantly higher than for a purely melt-pressed sample, presumably because of its enhanced self-adhesive strength [41]. Various rheological and NMR investigations proved that this rubber behaves like a nanophase-separated system consisting of a less mobile part (85%) with a T_g just below room temperature (corresponding to ongoing mechanical relaxation) and a more mobile part (15%). It was found that irreversible (chemical) crosslinking occurred above 110 °C, resulting in an aging effect and, therefore, in weakening of the self-healing ability [42].

2.3 Hydrogen Bonding Interactions Between Nucleobase Analogs and Tailor-Made Hydrogen Bonding Wedges

Several supramolecular polymers based on hydrogen bonding interactions between nucleobases and their analogs and tailor-made hydrogen bonding wedges have been described [25, 43–51]. The self-healing mechanism is often supported by a second

principle such as phase segregation phenomena or a second supramolecular interaction (e.g., π–π interactions) [26, 28, 52–56].

Self-healing polymers based on weak hydrogen bonding interactions were accomplished by the synthesis of bivalent PIBs functionalized with barbituric acid moieties and a Hamilton wedge [28] (Fig. 2b) and investigated via temperature-dependent melt rheology. The formation of dynamic supramolecular junction points was confirmed by rheological investigations showing terminal flow at low frequencies but a rubbery plateau zone at high frequencies. The occurrence of aggregation could be confirmed by small angle X-ray scattering (SAXS) measurements [26, 28]. Thus, strong and tough self-healing supramolecular polymers with an increased thermal stability were observed for barbituric acid telechelic PIBs, although their dimerization is very weak in solution (Fig. 5a). The self-healing behavior was related to thermoreversible formation of larger aggregates enhanced by microphase separation between the polar hydrogen bonding synthons and the nonpolar PIB backbone. Interestingly, the molar mass of the investigated polymers barely had an effect on the supramolecular bond lifetime or on the temperature-dependent viscosity behavior. Consequently, freshly cut pieces of PIBs modified with barbituric acid groups were completely healed within 48 h, suggesting application as a room temperature self-healing material (Fig. 5b). In contrast, PIBs bearing Hamilton wedges and barbituric acid moieties behaved like brittle rubbers. Consequently, terminal flow was only observed at temperatures above 100 °C [28].

This approach was extended to four-arm star-shaped polymers functionalized with thymine moieties to investigate the influence of polymer architecture on the strength of the supramolecular interaction and the subsequent self-healing performance, while keeping the density of supramolecular moieties approximately constant (Fig. 6) [56]. Although thymine motifs display an even lower dimerization tendency than barbiturate moieties in solution, neat four-arm star thymine-telechelic PIB behaved like a tough rubber with a prominent rubbery plateau at room temperature. In comparison with bivalent barbiturate-telechelic PIB, the observed plateau modulus (1.1×10^6 Pa) was higher, which was attributed to supramolecular cluster formation consisting of up to ten hydrogen bonding moieties, as demonstrated via SAXS investigations. Consequently, an increased supramolecular bond lifetime of $\tau_B = 67$ s was also observed. Self-healing occurred within 72 h at room temperature [56].

Four-arm star-shaped polymers have also been utilized for the preparation of interwoven network-structured self-healing materials, where the self-healing behavior is related to supramolecular clustering of hydrogen bonding moieties. These polymers are additionally reinforced by a covalent network formed via a CuAAC click reaction (Fig. 7). Hence, four-arm star-shaped polymers containing both thymine moieties and azide end groups have been prepared and crosslinked with a multivalent star-shaped alkyne-functionalized polymer [56].

Furthermore, the influence of the architecture on the dynamics of association and clustering, and therefore on the self-healing of supramolecular hydrogen-bonded polymers, was also investigated by preparing structurally simple supramolecular

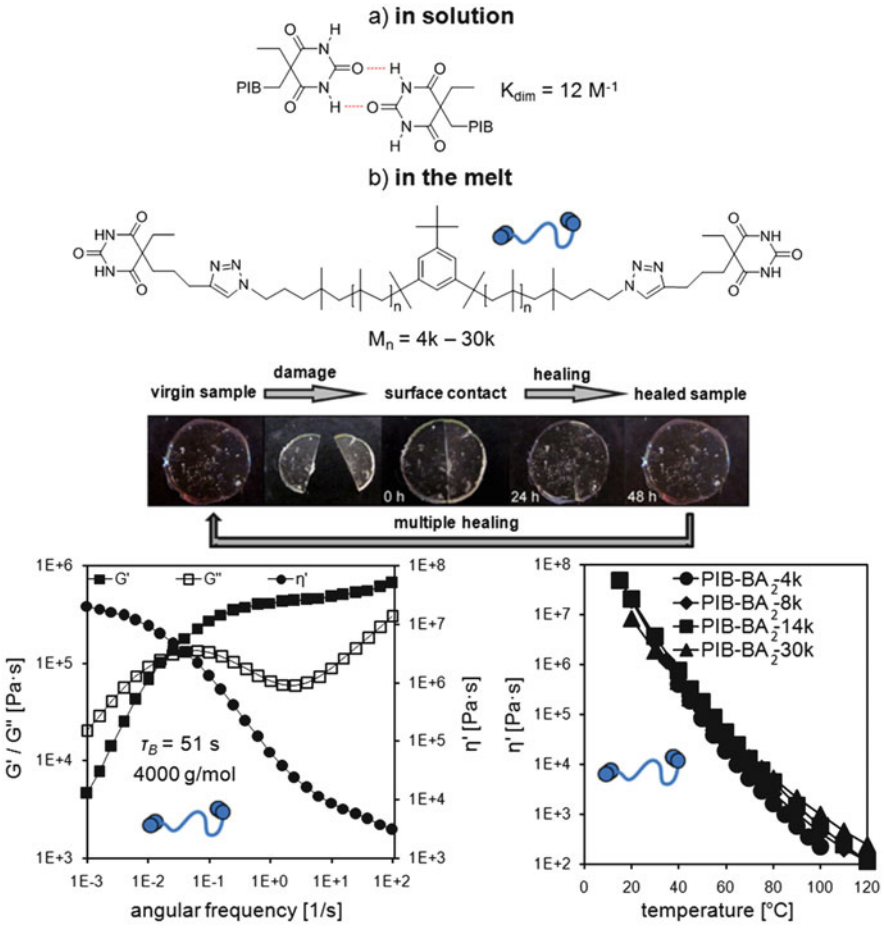

Fig. 5 (**a**) Dimerization of two PIB chains functionalized with barbiturate moieties (in solution: $K_{dim} = 12\ M^{-1}$). (**b**) Bivalent barbiturate-telechelic PIBs with molar masses of 4,000 – 30,000 g/mol show a self-healing response at room temperature as a result of formation of supramolecular clusters containing polar barbiturate moieties. The supramolecular bond lifetime for a bivalent barbiturate-telechelic PIB with a molar mass of 4,000 g/mol is $\tau_B = 51$ s (*bottom left*). The viscosity is unaffected by an increase in molar mass from 4,000 – 30,000 g/mol (*bottom right*). Figure reprinted and adopted from [28] with permission from The Royal Society of Chemistry (Copyright 2012)

PIB "graft" polymers with 1 mol% of a 4-pyridine substituted styrene monomer **1** (Fig. 8) [54]. Although, on average, less than one crosslinker per chain is present in PIB-**1** (2,800 g/mol), approximately two crosslinkers per chain were found in PIB-**1** (9,000 g/mol). Accordingly, only for polymers with a molar mass higher than 9,900 g/mol a formation of a rubbery plateau was observed related to weak supramolecular network formation as a result of the pyridine-N–H–N-pyridine bonds present (Fig. 8d). This was further proven by comparing the theoretical

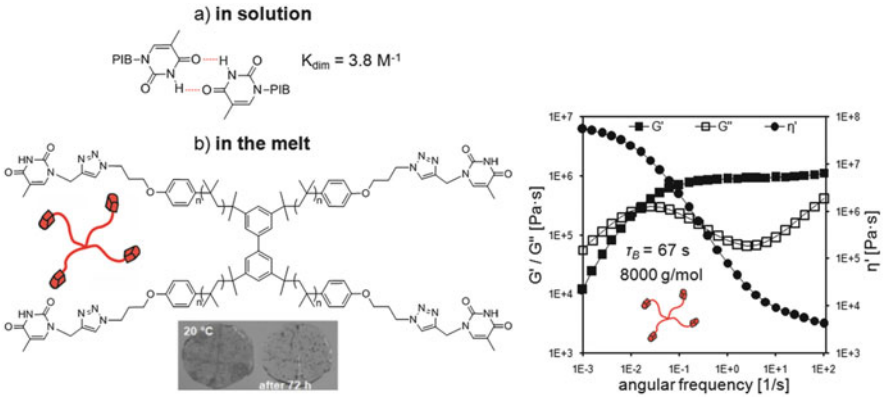

Fig. 6 (**a**) Dimerization of two PIB chains functionalized with thymine moieties (in solution: $K_{dim} = 3.8\ M^{-1}$). (**b**) Rheology of tetravalent star-shaped thymine-telechelic PIB with a molar mass of 8,000 g/mol and supramolecular bond lifetime of $\tau_B = 67$ s (right diagram) shows self-healing at room temperature. Figure reprinted and adopted with permission from [56] with permission from Elsevier Ltd. (Copyright 2015)

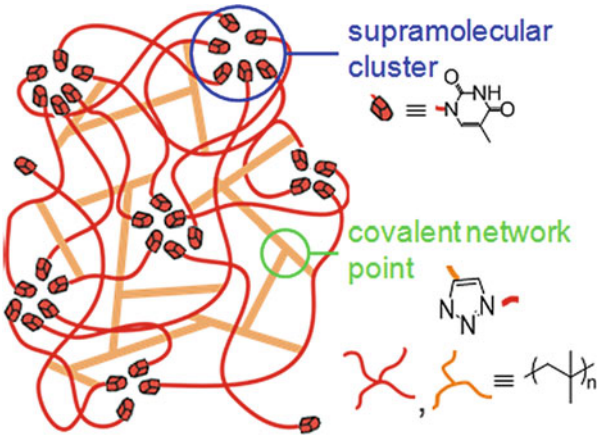

Fig. 7 Interwoven network structure composed of supramolecular clusters of thymine moieties and a covalent network created via a CuAAC click reaction between multivalent azide- and alkyne-functionalized star-shaped polymers. Figure reprinted and adopted from [9] with permission from Elsevier Ltd. (Copyright 2015)

segment length between two supramolecular crosslinking points ($M_{c\ theo}$) with the segment length determined via rheology measurements ($M_{c\ plat}$) [54].

The influence of molecular architecture on the self-healing behavior was probed by investigating V- and H-shaped supramolecular copolymers. For this purpose, a molecular design reminiscent of thermoplastic elastomers (TPEs) was utilized. Furthermore, the influence of the position of the hydrogen bonding moiety on the self-healing ability was investigated in detail (Fig. 9) [55]. Thus, a V-shaped

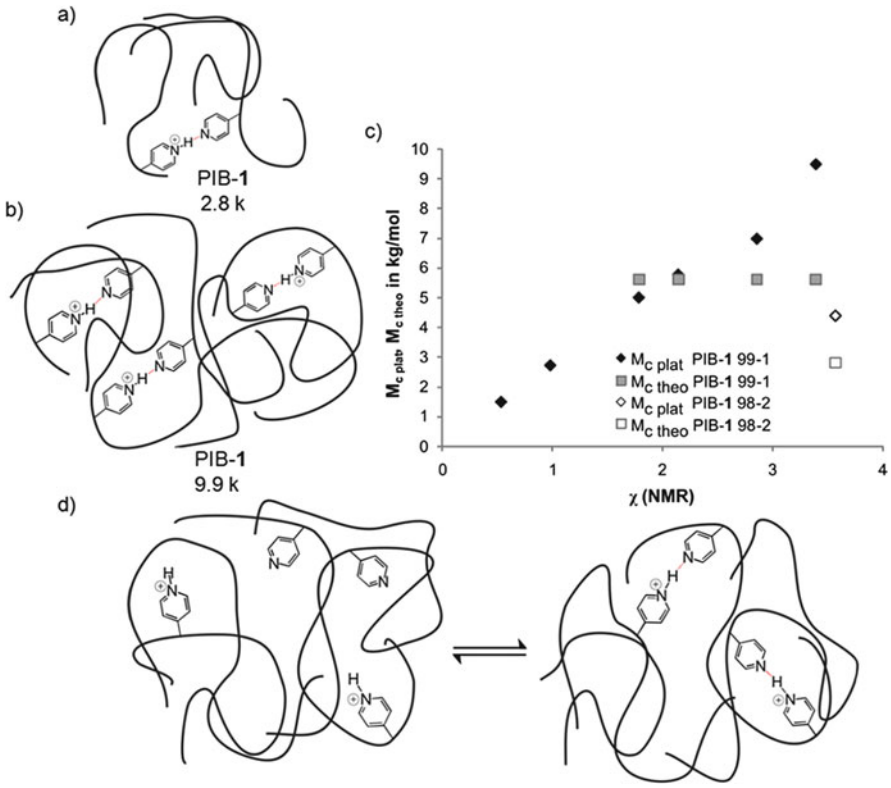

Fig. 8 PIB copolymers with 1 mol% of a 4-pyridine-substituted styrene monomer **1** with (**a**) molar mass of 2,800 g/mol (1.0% incorporation) or (**b**) molar mass of 9,900 g/mol (1.1% incorporation). (**c**) Comparison of the molar mass ($M_{c\ plat}$) between the incorporated supramolecular units **1** (determined via rheology measurements) and the theoretical segment length ($M_{c\ theo}$) between incorporated units **1** (determined via NMR investigations). χ is the number of comonomer **1** units per chain. (**d**) Equilibrium between aggregated/de-aggregated polymer chains. Figure reprinted and adopted from [54] with permission from John Wiley and Sons (Copyright 2012)

barbiturate-functionalized soft–hard–soft triblock copolymer, with the hydrogen bonding moiety located in the hard block to introduce an additional shape-persistence, was synthesized via reversible addition-fragmentation chain-transfer (RAFT) polymerization. The copolymer was blended with a complementary α,ω-Hamilton wedge telechelic isoprene to obtain an even more sophisticated polymer architecture. Both, the pure barbiturate-functionalized copolymer and the polymer blend showed a self-healing response at 30 °C, resulting in a 95% or 91% recovery of the original strain at break within 24 h, respectively. The V-shaped copolymer provided better mechanical properties as a result of the higher fraction of the hard block. These results demonstrate that polymer blends, fixed by matching hydrogen bonding moieties, can exert self-healing properties, which indicates a useful approach for tailoring material properties within a self-healing polymer [55].

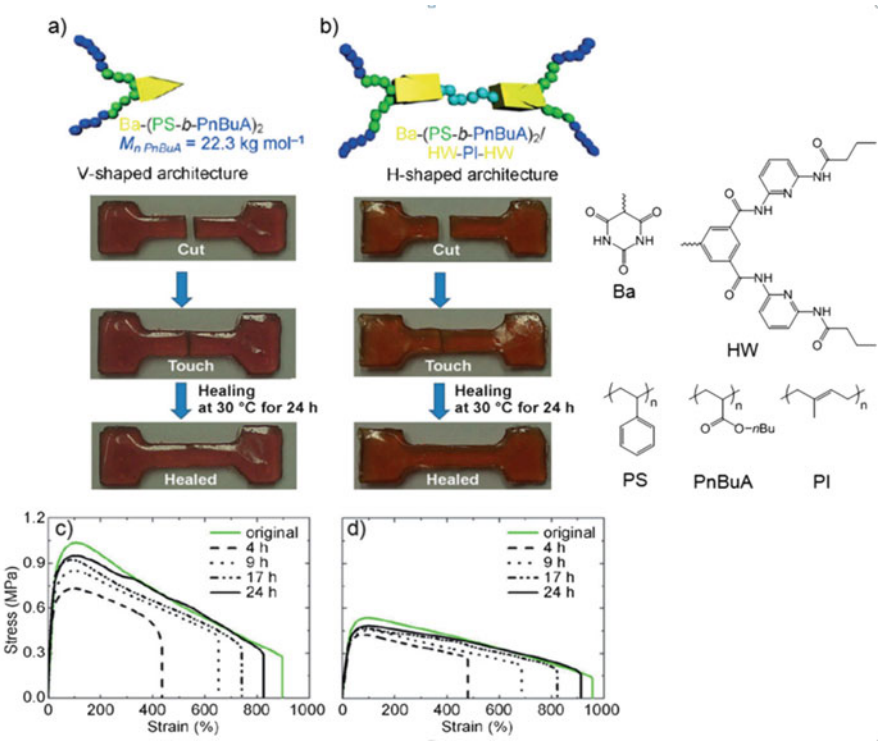

Fig. 9 (**a**) V-shaped barbiturate (Ba)-functionalized polymer blend (PS-*b*-PnBuA)$_2$ and (**b**) H-shaped polymer blends consisting of Ba-functionalized (PS-*b*-PnBuA)$_2$ and bivalent Hamilton-wedge (HW)-functionalized PI (2:1 blend) prepared via RAFT polymerization show self-healing at 30 °C within 24 h. (**c, d**) Tensile tests of pristine V-shaped Ba-functionalized (PS-*b*-PnBuA)$_2$ (**c**) and pristine H-shaped polymer blends consisting of Ba-functionalized (PS-*b*-PnBuA)$_2$ and bivalent HW-functionalized PI (**d**) after 4, 9, 17, and 24 h of self-healing. Figure reprinted and adopted from [55] with permission from John Wiley and Sons (Copyright 2015)

By investigating adenine-, thymine- and cytosine-modified low molar mass polyTHFs [52, 53] it was found that only the adenine- and the cytosine-terminated polymers demonstrated film- and fiber-forming capabilities as a result of hydrogen bonding interactions. As the supramolecular interactions presented are generally weak, it was assumed that a second driving force, namely π–π-stacking interactions of hard crystalline nucleobase chain ends in combination with phase segregation between the soft polymer backbone and the hard hydrogen bonding moieties, must have contributed to this self-assembly behavior [52, 53]. Applications of self-healing adenine-modified polyTHFs were reported, utilizing the temperature stability of the resulting supramolecular network structures up to 90–120 °C [53].

2.4 *Hydrogen Bonding Interactions Between Ureidopyrimidone Synthons*

Supramolecular polymers functionalized with ureidopyrimidone (UPy) moieties and their dynamic properties in solution have been intensely studied because of their high dimerization constant ($CHCl_3$, $K_{dim} = 10^6\ M^{-1}$) [57, 58]. Consequently, the generation of supramolecular polymers, polymer networks, or polymeric nanoparticles have been investigated in the bulk phase [59]. Furthermore, self-healable polymers as well as supramolecular rubbers based on UPy hydrogen bonding interactions have been commercialized under the trade names SupraB™ and Kraton® by SupraPolixBV [24, 60].

Thus, the phase separation of bivalent UPy-telechelic PEG (Fig. 10) in hydrophobic hydrogen bonding domains consisting of UPy moieties and the PEG backbone resulted in the formation of solid-like hydrogels. Self-healing of these materials was observed at 50 °C when the initial properties switched to those of a viscous liquid [61, 62].

The formation of supramolecular hydrogen-bonded polymer networks between trivalent UPy-functionalized PPE-PEO block copolymers and bivalent UPy-modified PDMS has been reported [23]. The resulting supramolecular crosslinked materials behaved similarly to entangled linear polymers. Both, gel formation in solution and crystallization in the bulk phase were observed as a result of the directionality of the supramolecular interactions [23]. Thus, UPy-telechelic PDMS formed TPEs with a rubbery plateau and a high activation enthalpy for stress relaxation [63, 64] caused by lateral stacking of UPy dimers additionally reinforced by π–π interactions. The observed aggregation behavior leading to assembly of spherical aggregates or fibers was attributed to the incompatibility of the hard block consisting of microcrystalline domains of associated UPy dimers and the soft

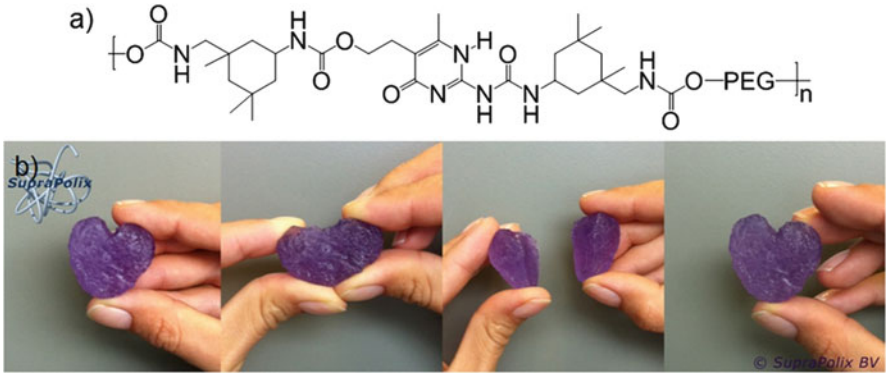

Fig. 10 (**a**) UPy-functionalized PEG. (**b**) Self-healing of an UPy-functionalized PEG heart (colored by adding a purple dye, 15 wt% in water): Initial heart shape was reestablished after pressing cut halves together. Figure reprinted and adopted from [61] with permission from SupraPolix BV and John Wiley and Sons (Copyright 2011)

PDMS backbone, leading to microphase separation [63, 64]. Similarly, UPy-telechelic poly(*n*-butyl acrylate) (P*n*BA), polystyrene (PS), and poly(butadiene) form micellar clusters of UPy aggregates in the solid state [65], comparable with observations for DAT/THY systems [25–27].

Investigations of crystalline UPy-modified poly(ethylene adipate) [66] showed that the self-healing performance depended on the junction unit between the polymer backbone and the hydrogen bonding moiety, proving the strong influence of even remote functional groups on the assembly of hydrogen bonds. Thus, self-healing at room temperature was observed for polymers containing hexamethylene linkers, related to slower recovery in crystallinity. In contrast, tolyl linkers allowed a faster recovery of crystallinity, while shifting the healing temperature above the melt temperature [66].

Bivalent UPy-telechelic perfluoropolyethers (PFPEs) [67] recovered their storage modulus within 2 min of shearing at 130 °C as a result of formation of hard crystalline UPy domains based on phase separation between the soft polymer backbone and the hydrogen bonding moieties. In contrast, PFPEs functionalized with alkylated UPy groups showed suppressed crystallization, resulting in an increased recovery time of the storage modulus of 18 min after shearing at 110 °C [67] (Fig. 11).

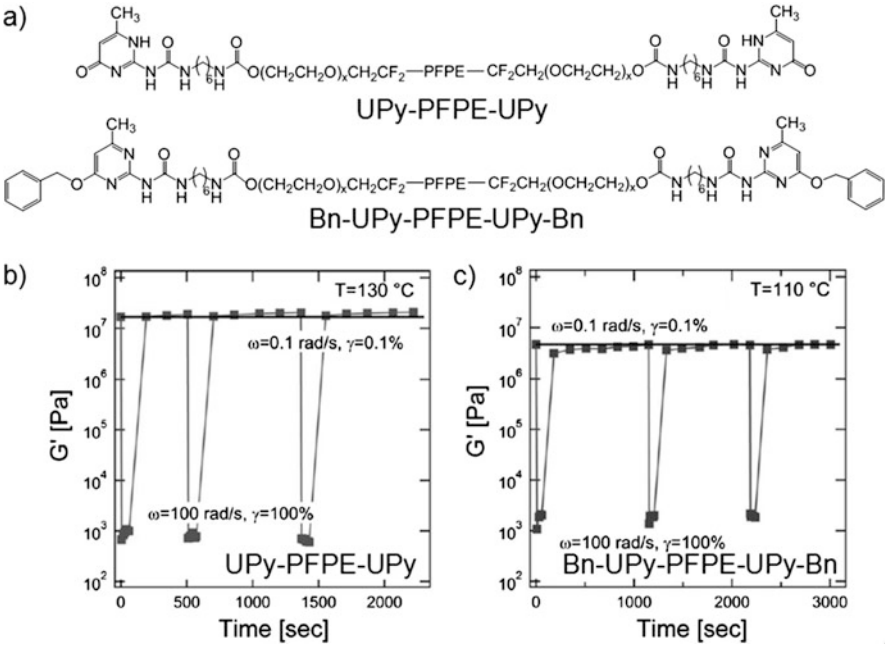

Fig. 11 (**a**) Structures of bivalent UPy-telechelic PFPE and bivalent Bn-UPy-telechelic PFPE. (**b**, **c**) Multiple deformation-recovery cycles of bivalent UPy-telechelic PFPE (**b**) and bivalent Bn-UPy-telechelic PFPE (**c**). Figure reprinted from [67] with permission from John Wiley and Sons (Copyright 2013)

In bivalent UPy-modified polycaprolactone (PCL), stacking of UPy dimers supported by hydrogen bonding interactions between urethane linker groups was observed, however, chain scission proceeded faster than reptation. The materials obtained showed a rubber plateau zone even at low frequencies and viscous flow as a result of supramolecular network formation [68]. In contrast, no rubbery plateau was observed for tri- and tetravalent UPy-urethane modified PCLs because the crystallization and stacking of UPy dimers was prevented by the polymer architecture, resulting in a too-short lifetime of the supramolecular network [69]. Similarly, large and bulky substituents interfered with supramolecular assembly due to steric hindrance [68].

By comparing copolymers composed of *n*-butyl acrylate (*n*BA) and an UPy-functionalized acrylate, acrylamidopyridine, acrylic acid, or carboxyethylacrylate [70], it was found that copolymers containing weak hydrogen bonding interactions behaved like un-entangled melts, with hydrogen bonding dynamics faster than rheological chain relaxation. In contrast, copolymers with strong hydrogen bonding interactions behaved like entangled polymer networks, resulting in soft and elastic solids. Flow activation energies increased linearly with increasing amount of hydrogen bonding moieties showing a dimer lifetime longer than 10 s [70]. Thus, copolymers prepared from poly(2-ethylhexyl methacrylate) and an UPy-modified methacrylate revealed an increase in complex viscosity as well as an increase and a lengthening of the plateau modulus with increasing UPy content [71]. Similar copolymers composed of *n*BA and UPy-functionalized acrylate (UPy content of 7.2%) showed a recovery of the self-adhesion strength of fractured surfaces up to 100% after a healing time of 50 h [72].

TPEs with a prominent plateau modulus and with bulk properties depending on the distance between stacked aggregates of UPy dimers were obtained by copolymerizing UPy-modified *n*BA with a Boc-protected amine-functionalized monomer [73]. With increasing UPy content, a linear increase in the plateau modulus was observed. The effective bond lifetime of hydrogen-bonded aggregates increased, proving that every UPy side group was active within the network for UPy contents of 7 mol% or higher [73]. Similarly, the formation of soft rubbers or TPEs was observed for bivalent UPy-modified poly(ethylene butylene)s [74]; multifunctionalized poly(ethylene butylene)s carrying urethane, urea, and UPy groups [75, 76]; and UPy-functionalized amorphous polyesters [77].

UPy-functionalized poly(urethane)s [78] also found application as stress-sensing systems by incorporating spiropyran units into the polymer backbone, enabling stress-induced ring-opening that resulted in the merocyanine form, visualized by a color change. Furthermore, UPy-modified polymers able to dissipate strain energy were used to mimic the modular structure within titin, as the dissociation of hard UPy domains consisting of stacked dimers is similar to the unfolding process of sacrificial bonds in modular biomacromolecules [78]. Thus, a titin-mimicking modular polymer with high toughness and adaptive behavior, including self-healing ability, demonstrated full recovery of toughness and strength at 80 °C within 30 s [79].

2.5 Hydrogen Bonding Interactions Between Acid-, Phenyl Urazole Acid- or Phenyl Urazole-Functionalized Polymers

Urazole moieties belong to the first generation of investigated supramolecular moieties incorporating dynamic (thermoreversible) properties into bulk butadiene polymers [17–20, 80], thereby guiding the later design of self-healing rubbers [21, 81, 82]. Viscoelastic properties [80] and a self-healing response were introduced into a thermoplastic material by reversible association of weak urazole motifs, resulting in multiphased structures as a result of phase separation effects [83, 84]. As a consequence, time–temperature superposition of rheological data was impossible even for low concentrations of hydrogen bonding synthons [84], which was indicative of the strong effect of the few "weak" hydrogen bonds on the recovery of material properties after applied stress [85, 86]. As a result of the formation of hydrogen bonding interactions, related to hindrance of local flow processes, a broadening of the relaxation time up to seconds was observed. Furthermore, an increase in the activation enthalpy was attributed to an increasing degree of functionalization and, thus, to the formation of supramolecular clusters with higher stability [85–87].

4-Urazoylbenzoic acid-modified bivalent PIBs [19, 88] able to form hydrogen-bonded dimers revealed melting of ordered hydrogen bonding clusters at 110–120 °C. Within this temperature range a transition from elastic to viscous behavior was observed, related to the reorientation and breaking of ordered supramolecular clusters into disordered multiplets of associated hydrogen bonding chains. As expected, the time–temperature superposition failed and stress relaxation within the polymer was attributed to the relaxation of multiplets and deformation of supramolecular clusters [19, 88].

2.6 Bis(urea)-Based Hydrogen Bonding Interactions

Urea-based hydrogen bonds are one of the simplest systems for introducing dynamic properties into a polymer, as the synthesis only requires a reaction between isocyanate and amine building blocks, which are widely available in polymer technology.

Thus, P*n*BAs functionalized with a bis(urea) group in the middle showed viscoelastic properties. The viscosity increased with decreasing molar mass up to 20,000 g/mol, which was attributed to hydrogen bonding interactions completely determining the rheological properties. In contrast, for functionalized P*n*BAs with a molar mass higher than 20,000 g/mol, the polymers behaved almost like unfunctionalized high molar mass P*n*BAs. Their rheology was controlled by polymer dynamics, while incorporated supramolecular binding motifs simply increased the terminal relaxation time as a result of hydrogen bonding interactions [89].

Similarly, PDMS grafted with bis(urea) moieties formed TPEs as a result of supramolecular crosslinking related to (partial) self-organization of incorporated bis(urea) units in crystal-like domains [90]. Investigations of poly(urethane)-based TPEs containing a soft poly(ethylene-*co*-butylene) middle block [91] showed that an increase in microphase separation in the bulk led to an increased hydrogen bonding potential. Thus, an increase in the scattering intensity in SAXS experiments and an increase in the storage modulus were observed when the end group changed in the order dibutyl < morpholine < diol [91]. Polyurea-urethanes with triuret blocks displayed a crosslinked structure at room temperature as a result of hydrogen bonding interactions, whereas de-crosslinking was observed between 105 and 135 °C [92]. In contrast, tetrauret block-containing polyurea-urethanes resulted in a folded structure as a result of the zigzag conformation, with a higher thermal stability up to 170–190 °C [92].

Single- or double-stranded structures were also observed for self-healing supramolecular silicones prepared by crosslinking of tris(urea)-modified PDMS with hydrazine units [93] via sextuple hydrogen bonding interactions. These materials revealed a self-healing ability when cut films were reassembled immediately, whereas no self-healing behavior was observed after keeping cut surfaces apart for more than 10 min as a result of equilibrating and reassembling of hydrogen bonding moieties [93].

Low molar mass bis(urea) moieties as well as PIBs containing bis(urea) functionalities within the polymer backbone formed comb-shaped supramolecular assemblies at room temperature, resulting in the formation of filaments or tubes. The length of the tubes could be tuned by varying the concentration and/or the solvent [94, 95]. The supramolecular association present strongly influences the bulk properties and, therefore, the self-healing ability within the bulk material could be estimated as a result of the dissipative nature upon deformation [95, 96]. The investigated polymers showed a self-organization behavior over a timescale of days, resulting in viscoelastic soft gels at room temperature, which disrupted at 80 °C but retrieved their structure after 20 h of annealing, highlighting their potential as dissipative soft adhesives and self-healing materials [96].

Similarly, low molar mass *N*,*N*′-disubstituted ureas formed supramolecular polymers comparable to high molar mass poly(urethane)s and behaved like organogels, showing viscoelastic properties and a relaxation time of several seconds [97–99].

2.7 *Hydrogen Bonding Interactions Between 2,7-Diamido-1,8-naphthyridine Synthons and Ureidopyrimidone, Ureido-7-deazaguanine, or the Butylurea of Guanosine*

By investigating 2,7-diamido-1,8-naphthyridine (DAN) and UPy end-functionalized P*n*BAs and poly(benzyl methacrylate)s it was found that the phase behavior and microstructure in the bulk were controlled by hydrogen bonding interactions [100]

as well as by temperature changes, directly influencing the compatibility of the phases [101]. Thus, UPy dimerization led to compatibilization, whereas complementary hydrogen bonding interactions resulted in significant reduction in macroscopic phase separation [100] and in the formation of supramolecular diblock copolymers [101] or graft polymers [102].

Supramolecular alternating copolymers were formed by hydrogen bonding interactions between a 1:1 mixture of a bis-UPy-functionalized polyTHF and a bis-DAN-functionalized low molar mass linker [103]. By increasing the bis-DAN linker content, the virtual degree of polymerization decreased because the bis-DAN linker acted as a chain stopper [103]. Accordingly, the concentration dependence of the virtual degree of polymerization and, thus, the chain length can be blocked in a defined concentration range by the use of chain stoppers, which enables conclusions to be drawn about the hydrogen bonding interaction corrected for concentration effects [104–106]. In contrast, in the case of weaker hydrogen bonding interactions in urea-modified polyether polyols, no break-up of the supramolecular assembly was observed because the polymer ends were incorporated in the microphase-separated hydrogen bonding arrays, resulting in the formation of phase-separated TPEs [107].

The hydrogen bonding interactions between ureido-7-deazaguanine (DeUG) and DAN as well as between the butylurea of guanosine (UG) and DAN have been intensely studied in solution [108–112]. It was found that DAN revealed a redox-responsive behavior and, therefore, a chemically and electrochemically switchable high affinity for DeUG in its reduced form and a low affinity for the oxidized form of DeUG. This characteristic might be interesting and applicable for tailoring self-healing applications, because the on–off switch ability has already found use in the control of supramolecular network formation [113].

3 Self-Healing by π–π Stacking Interactions

π–π stacking interactions in non-hydrophilic environments are among the most important supramolecular interactions, although rated significantly weaker in strength than hydrogen bonds or ionic interactions [114]. Usually, association constants for simple π–π systems are ~10^2 M^{-1}, with some values just exceeding 10^3 M^{-1} [115]. Basically, the conventional π–π stacking systems of, for example, pure aromatic rings are too weak to enable a significant healing effect and, thus, are not suitable (e.g., PS is not a self-healing polymer below its T_g). A literature study revealed the use of multivalent "stacked" or chain-folded π-systems (Fig. 12) as significantly more stable supramolecular systems. Thus, careful molecular design of π–π-stacking [117] (Table 1, entry 1), mostly induced via the formation of stacked charge-transfer structures, can lead to significantly enhanced association constants, even reaching association constants ranging from ~11,000 M^{-1} [118] to ~100,000 M^{-1} (Fig. 12c) [116, 119]. Thus, the use of multivalent electron-deficient naphthalene diimide units in a polymer chain, together with suitably planned

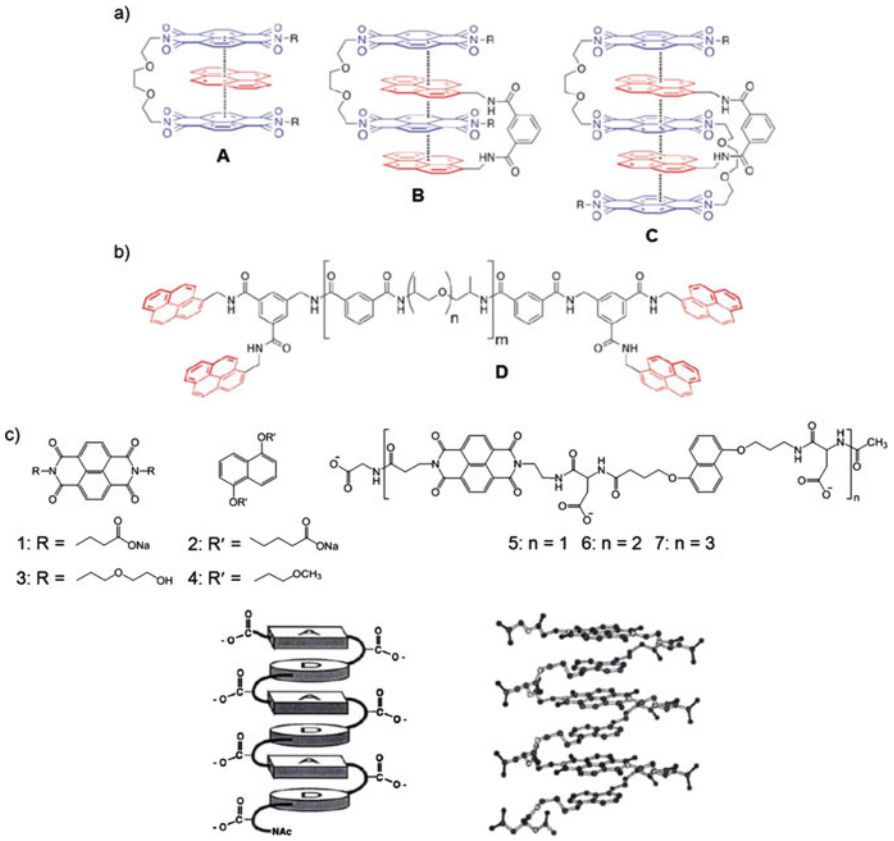

Fig. 12 (**a**) Examples of π–π complexes *A*–*C* formed between naphthalene diimide oligomers (*blue*) and pyrene or a tweezer-type pyrene-derivative (*red*) containing two to four face-to-face π–π stacking interactions. K_a values are 130, 3.50×10^3, and 11.0×10^3 M^{-1} for π–π complexes A, B, and C, respectively. (**b**) Structure of a bis-tweezer-type pyrene-end-capped polyamide D. (**c**) 1,5-Dialkoxynaphthalenes and 1,4,5,8-naphthalenetetracarboxylic diimides as aromatic donor and acceptor units. A pleated secondary structural element based on donor–acceptor interactions is formed: schematic representation (*bottom left*) and computer-generated representation (*bottom right*). Figure reprinted and adopted with permission from [116] (Copyright (2011) American Chemical Society) and from [117] (Copyright 1995, Rights Managed by Nature Publishing Group)

tweezer-like electron-rich bipyrenyl end groups (Table 1, entries 2, 3, and 5–9) can lead to strongly enhanced binding constants, additionally supported by the formation of hydrogen bonding interactions between the amide groups of the naphthalene diimide-modified acceptors and the carbonyl groups of the pyrenyl-functionalized donors (Fig. 12a, b) [118–125, 127].

The reversibility [134] of such supramolecular bonds can enable the design of a reversible healing system that is able to heal after overcoming the required activation energies, in turn achieving reorganization of (polymer) chains and resulting in healing. A significant number of different self-healing systems at elevated

Table 1 Summary of π–π stacking interactions utilized for the design of self-healing

Entry number	Donor (D) moiety	Acceptor (A) moiety	Polymer	Healing temperature/ °C	References
1	Dialkoxynaphthalenes	Naphthalene tetracarboxylic diimides	–	–[a]	[117]
2	Pyrenyl/tweezer-type pyrenyl units	Naphthalene tetracarboxylic diimide units	–	–[a]	[118]
3	Pyrene-end-capped/bis-tweezer-type pyrene-end-capped	Naphthalene diimide units	D: polyamide A: PEO-PPO copolymer	140	[116]
4	Pyrenyl units	Naphthalene tetracarboxylic diimide units	PEO (all-in-one system)	–[a]	[119]
5	Tweezer-type pyrenyl units	Pyromellitimide units /4,4′-bi-phenylenedisulfone units/naphthalene tetracarboxylic diimide units	D: – A: macrocyclic ether-imide-sulfones	–[a]	[120]
6	Tweezer-type pyrenyl units	Pyromellitimide units/4,4′-bi-phenylenedisulfone units	D: – A: macrocyclic ether-imide-sulfones/poly (imide)s	–[a]	[121]
7	Tweezer-type pyrenyl units	Pyromellitimide units/4,4′-bi-phenylenedisulfone units	D: – A: poly(imide)s-	–[a]	[122]
8	Tweezer-type pyrenyl units	Pyromellitimide units/4,4′-bi-phenylenedisulfone units/naphthalene tetracarboxylic diimide units	D: – A: poly(imide)s	–[a]	[123]
9	Tweezer-type pyrenyl units	Pyromellitimide units/4,4′-bi-phenylenedisulfone units/naphthalene tetracarboxylic diimide units	D: – A: macrocyclic ether-imide-sulfones/poly (imide)s	–[a]	[124]
10	Pyrene-end-capped	Naphthalene tetracarboxylic diimide units	D: polysiloxane A: PEO	≈100	[125]
11	Pyrene-end-capped	Naphthalene tetracarboxylic diimide units	D: polyamide A: PEO-PPO copolymer	≥50	[126]

12	Pyrene-end-capped	Naphthalene tetracarboxylic diimide units	D: polybutadiene A: PEO-PPO copolymer	≈100	[127]
13	Pyrene-end-capped	Naphthalene tetracarboxylic diimide units	D: PEO A: PEO-PPO copolymer	75–100	[128, 129]
14	Pyrene-end-capped/perylene-end-capped	Naphthalene tetracarboxylic diimide units	D: PEO A: PEO-PPO copolymer	≥75	[130]
15	Pyrene-end-capped	Naphthalene diimide units	D: polyamide A: PEO-PPO copolymer + cellulose nanocrystalls	≥65	[131]
16	Pyrene-functionalized gold nanoparticles	Naphthalene diimide units	D: – A: PEO	–[a]	[132]
17	Pyrene-end-capped + pyrene-functionalized gold nanoparticles	Naphthalene diimide units	D: polyamide A: PEO-PPO copolymer	≈75	[133]

[a]No healing temperature reported

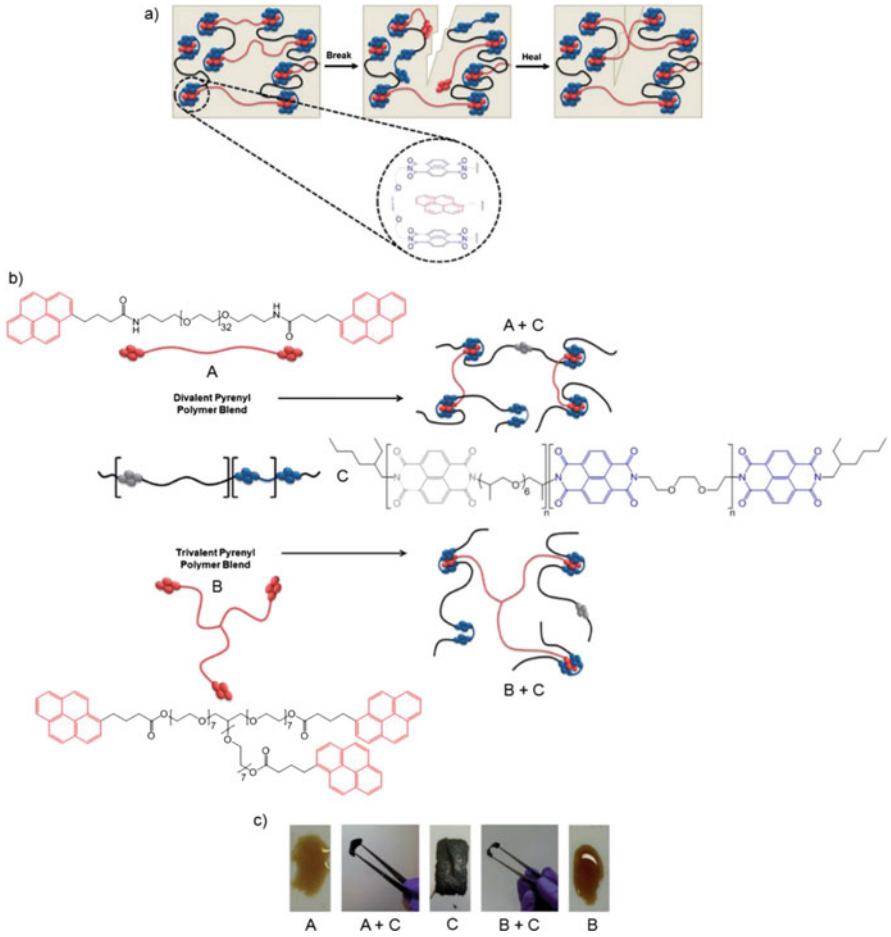

Fig. 13 (**a**) Complementary π–π stacking in polymer blends based on a π-electron-deficient naphthalene diimide unit (*blue*) and a π-electron-rich pyrenyl unit (*red*). In the case of a damage event, the π–π complex is disrupted and shows a self-healing response upon heating. (**b**) Formation of supramolecular polymer blends based on π–π stacking interactions between a π-electron-rich divalent or trivalent pyrenyl-terminated PEG (*red*, A or B) and a chain-folding naphthalene diimide-containing copolymer (*grey*/*blue*, C). (**c**) Polymer films of A, B and C and polymer blends of A + C and B + C cast from 2,2,2-trichlorethanol (dried at room temperature for 24 h, at 40 °C for 24 h and subsequently heated to 80 °C for 24 h). Figure reprinted from [128] with permission from The Royal Society of Chemistry (Copyright 2014)

temperatures (75 °C or above) have been designed, leading to reversible healing of polymer systems [116, 118–133, 135–140] (Fig. 13 and Table 1). Based on the suitable placement of the (multi)aromatic rings as well as on additional clustering effects of the aromatic units (segregating from the incompatible polymer chains) and the usually high activation barrier of (multi)aromatic interactions, healing of a polymeric material under high thermal loads can be achieved.

One of the first systems displaying self-healing via purely π–π stacking interactions was reported by the group of Hayes, relying on a relatively simple supramolecular blend containing naphthalene tetracarboxylic diimides and a pyrene molecule [125] (Table 1). PDMS polymers were utilized in these blends, which showed self-healing behavior at temperatures of ~115 °C (Table 1, entry 10). The concept was further extended to mixtures of two different polymers (Fig. 13 and Table 1, entries 11–13), where a multivalent poly(naphthalene tetracarboxylic diimide) polymer was mixed with bi- and trivalent pyrenyl-functionalized polymers [126–128], again displaying healing effects at elevated temperatures (200 °C, some starting at ~50 °C) [128]. In many of these examples, the tensile modulus recovered up to 95% of the initial value [127], also indicating the contribution of multivalency effects [128], leading to a higher tensile strength of the final material [130].

A significant contribution to self-healing using these naphthalene tetracarboxylic diimide/pyrene systems is also given by cluster formation. Clusters with a size of ~10 nm were detected via SAXS [128]. Presumably, self-healing is based on the cluster formation, because there is no direct linear correlation between the strength of the supramolecular interaction and the healing temperature or efficiency.

An extension of these systems towards self-healing nanocomposites was enabled by embedding cellulose nanocrystals with an aspect ratio of ~80 (Table 1, entry 15) [131] or Au nanoparticles (Table 1, entries 16 and 17) [132, 133] bearing pyrene functionalities on their surface. Whereas the cellulose whiskers served as a pure reinforcing element, the Au nanoparticles acted as an additional thermoresponsive element, facilitating healing by thermal activation. In both cases, percolating networks of the embedded filler systems were observed (cellulose whiskers at more than 10%) [131], together with the clustering effects of the Au nanoparticles (added amount 10–15%) [132, 133]. Although the addition of such large amounts of fillers led to a strongly reduced healing efficiency at the same temperature, presumably as a result of formation of percolated nanoparticle networks, which strongly reduced polymer dynamics and, thus, healing. Overall, despite the relatively simple concept, self-healing within π–π based systems takes place at comparable high temperatures (often more than 100 °C), placing the quest for still lower healing temperatures within the future prospects of development.

4 Self-Healing Ionomers

Compared with the relatively weak π–π-interactions and hydrogen bonds, ionic interactions show a higher aggregation strength. In general, ionomers are a subgroup of polymeric material that bear up to 15 mol% of ionic groups within the polymer. These groups can be distributed randomly as pendant groups or well-ordered in block copolymer-like architectures. They can also be located in the side chains or act as end groups [141]. The most common pendant ionic group for self-healing applications is a carboxylate group neutralized with sodium or zinc ions [142–145]. Unsaturated monomers containing carboxylate groups can be

polymerized via radical polymerization techniques. Afterwards, the unsaturated anions require neutralization with the desired metal counterion to provide the ionic character of the ionomers [146].

Compared with nonionic polymers, the introduction of ionic groups leads to significant changes in polymer properties (i.e. thermal and mechanical characteristics) as a result of new inter- and intramolecular interactions [147]. To explain these unique changes, several models of the inner structure of ionomers have been suggested. The multiplet-cluster model (Eisenberg–Hird–Moore or EHM model), which is briefly explained next, is one of the most accepted and reported models for how ionic groups influence the morphology of these materials [22]. In general, ionic groups (hydrophilic) show phase separation from the surrounding polymer matrix (hydrophobic) because of the low dielectric constant and the low T_g of the matrix [141, 148]. This phase separation leads to aggregation of a certain number of ion pairs, called multiplets, in which the ion pairs closely interact. On the one hand, electrostatic interactions of the ion pairs and, on the other hand, elastic forces of the attached polymer chains affect the formation of these multiplets as well as their size [22, 149]. A schematic representation of such a multiplet is depicted in Fig. 14 for a poly(styrene-*co*-sodium methacrylate) ionomer. The multiplet in the inner dashed

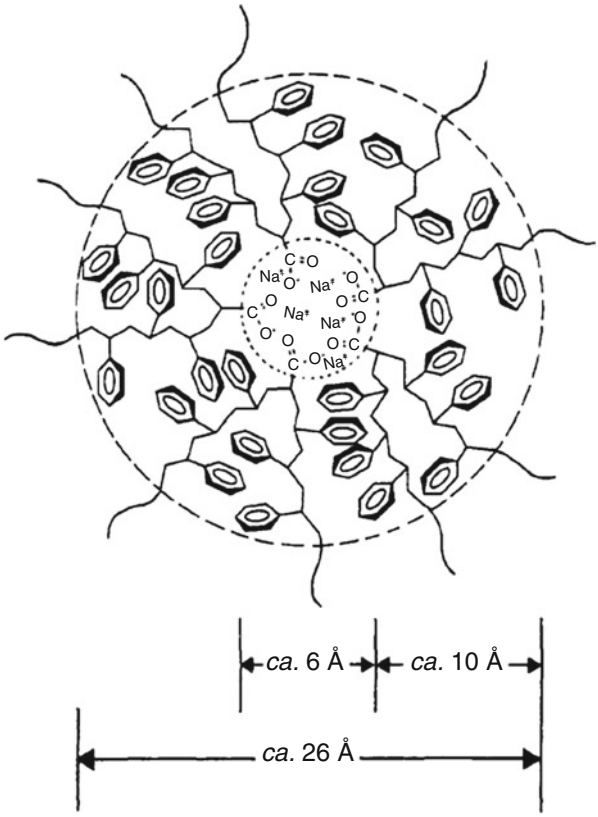

Fig. 14 Multiplet (*inner dashed circle*) surrounded by the region of restricted mobility (between *inner* and *outer dashed circles*), according to the multiplet-cluster model (reprinted with permission from [22])

circle is completely surrounded by the polymer matrix. These fixed points influence the region between the two dashed circles. Here, the polymer chains have reduced mobility compared with the outside, where the undisturbed polymer mobility is present. Furthermore, the multiplets can form clusters beyond a minimum ion concentration. Thereby, only the regions of restricted mobility overlap and, if the overlap is large enough, a phase-separated region is generated, which leads to an additional (higher) T_g of the material [22].

Besides this well-established concept, there are also publications that describe the behavior of ionomers in a different fashion [150–152]. Han and Williams used Fourier transform infrared (FTIR) spectroscopy to investigate poly(ethylene-*co*-methacrylic acid) copolymers (EMAA) containing several metal ions [153]. The authors proposed two different mechanisms for the formation of ionomers. The first mechanism is described by the existing multiplet-cluster model, which is only applicable for ionomers based on alkali and alkaline earth metals. Ionomers with transition metal ions can be described with the specific coordinated complex model. In this model the different coordination structures are considered.

As mentioned above, the ionic content significantly influences the properties of the polymer and also plays a key role in later self-healing applications. Tadano et al. investigated the thermal properties of ionomers (EMAA) and demonstrated that the ionic clusters undergo an order–disorder transition [148]. At room temperature three phases are present: ionic clusters, a crystalline domain (i.e. polyethylene), and an amorphous domain (Fig. 15). By increasing the temperature, the ordered character of the ionic cluster disappears at a certain temperature T_i. At this point, the disordered state is present. During further heating, the polyethylene crystals melt at the melting point T_m. After cooling from above T_m, the molten polyethylene recrystallizes at T_c. Further cooling to room temperature does not

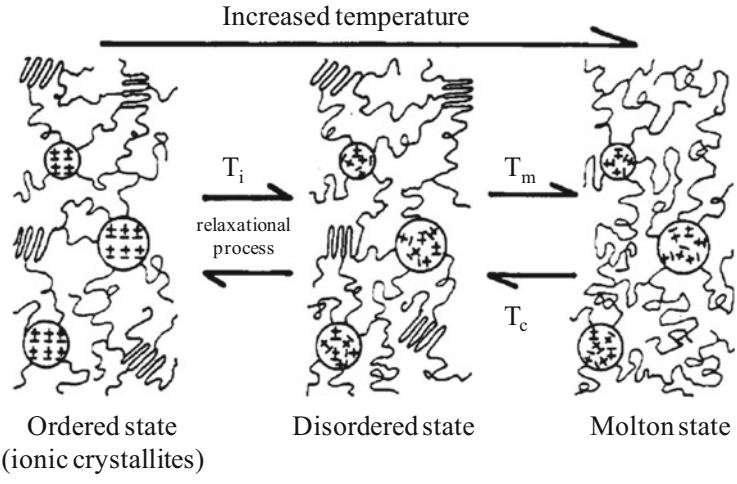

Fig. 15 Model of the order–disorder transition of clusters in ionomers and melting of the polyethylene domain during heating (reprinted with permission from [148])

result in any spontaneous transition of the ionic cluster. However, it was shown that re-formation of the ionic cluster takes approximately 38 days.

4.1 Self-Healing Under Ballistic Impact

Compared with nonionic polymers, ionomers have improved tensile strength, fracture resistance, toughness, and flexibility [8, 154]. The properties of the ionomers depend on their material structure, which is strongly influenced by the utilized ion pairs, the ion content (neutralization level), and the elastic behavior of the main chain [148, 153, 155].

Thermoplastic EMAA copolymers (Scheme 1) have been widely investigated for self-healing under ballistic impact [144, 145, 156–159]. Commercially available nonionic copolymers (Nucrel®) (http://www.dupont.com/products-and-services/plastics-polymers-resins/ethylene-copolymers/brands/nucrel-ethylene-acrylic-acid.html) and ionomers (Surlyn®) [26, 160] have mainly been investigated. The sodium ionomers differ in their neutralization levels (Surlyn 8940 with 30% and Surlyn 8920 with 60% neutralized acid groups). The ionomers provide excellent clarity, high toughness, and high stiffness, enabling a variety of different applications (e.g., food, cosmetics and medical device packaging, coatings for golf balls or ski boots) [161]. The self-healing behavior of these commercial materials has been tested in detail over the last two decades, equipped with the range of properties, knowledge about the materials, and their easy availability.

Fundamental work from both Fall and Kalista have shown the potential for self-healing after damage by high impact (i.e. ballistic penetration) [162, 163]. Thin films of EMAA materials were bombarded with projectiles, which completely passed through the material. After damage, the resulting hole closed very fast and only a small scar at the puncture site remained. These findings started several investigations on utilizing this unique self-healing capacity for healing layers in space vessels and navy aircraft fuel tanks or in medical applications [162, 164–166]. To optimize the self-healing ability, an understanding of the healing process including the mechanism is required. In the early state, the basic model describes the reversibility of the ionic interactions (i.e., physical crosslinks) as playing a key role in the ability to self-repair after a damage event. In addition, the free acid functions can form hydrogen bonds as a second form of reversible crosslink

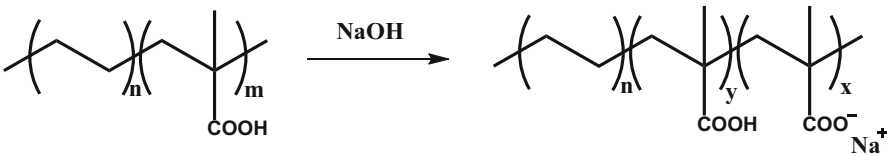

Scheme 1 Synthesis of the sodium ionomers of poly(ethylene-*co*-methacrylate acid) (EMAA) ($x + y = m$)

[146, 154, 167]. Kalista et al. investigated several ionomers and non-ionomers of EMAA and demonstrated that the ionic content does not correlate with the self-healing efficiency [168]. Nonionic EMAA polymers also showed self-healing behavior, whereas higher neutralized ionomers (e.g., Surlyn 8920) featured decreased self-healing capacity. Consequently, an alternative mechanism was proposed: hydrogen bonds present in nonionic Nucrel act as reversible crosslinks and enable self-healing properties [144, 146].

It has been proposed that a two-stage mechanism/healing process takes place after the projectile goes through the material [165, 168]. During impact, the material close to the bullet hole is heated to temperatures of approximately 92 °C (above the melting temperature) as a result of viscous dissipation [162]. This effect was also recently proven by Haase et al. using dynamic puncture tests [169]. After the projectile has passed through the material, the elastic properties of the materials cause a "flip back" of the polymer to the pre-impact position during the first stage. The molten polymer in the impact zone now has the possibility to rebound and close the hole. The subsequent slow second stage results in a completely sealed film through reorganization of the polymer chains (Fig. 16). Consequently, the unique combination of elastic rebound and viscous reflow of EMAA copolymers and other ionomers enables the self-healing response [159, 165, 168].

Further studies investigated different parameters of the ballistic and environmental conditions to learn more about the self-healing process and gain a deeper understanding of the underlying mechanism. Kalista et al. investigated the self-healing behavior after different damage types, including sawing, cutting, and nail puncture [165]. Cutting does not enable a later rebound of the two fragments. In contrast, the sawed samples featured self-healing properties as a result of the higher energy impact generated by frictional processes during sawing. Nevertheless, a higher energy impact is required to achieve effective self-healing behavior. Therefore, ballistic conditions were further investigated with respect to their thermal response and the so-initiated self-healing process. The self-healing capacities of ionomer films were tested over a range of temperatures. Heating the film reduced its

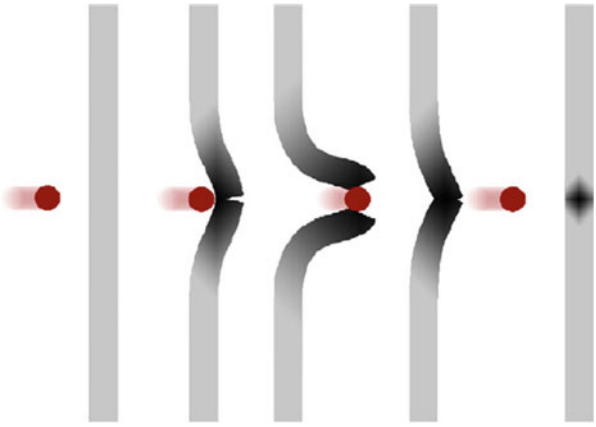

Fig. 16 Self-healing of ionomers after high-energy impact during ballistic penetration (reprinted with permission from [159])

elastic ability to return to its initial position after ballistic puncture. Thus, temperatures above 60 °C resulted in obstruction of the healing [144, 165]. To investigate the behavior of EMAA films at room temperature, Kalista et al. cooled the samples to 10, −10, and −30 °C, respectively. The authors found that self-healing is possible even at low temperatures. As a result of the two-stage mechanism, the local area around the puncture zone has to melt to achieve complete hole closure. Hence, a larger temperature rise is required for samples starting at −30 °C. Nucrel 925 was the only sample that did not heal at −30 °C, because of the formation of a brittle puncture zone resulting in a nonelastic behavior after ballistic penetration [165].

In 2008, Varley and van der Zwaag reported a new method for investigating the self-healing behavior of EMAA ionomers after ballistic treatment [159]. The method imitates the bombardment of a projectile by the utilization of a modified hydraulic tensile testing apparatus. Hereby, a disk-shaped object attached to a rod was pulled in a controlled manner out of the probe. Furthermore, the tool enabled quantitative information to be obtained about the healing process, because the damaging object is heatable and can be pulled at different velocities. The findings correlate with the proposed two-stage mechanism. Later, Varley and van der Zwaag intensively studied the ionomer Surlyn 8940 with this method [156, 167, 170]. In addition, the authors investigated the influence on the self-healing process of using different projectiles of varying size, weight, shape, and velocity. Self-healing behavior was achieved for all tested parameters. Although the impact morphologies showed differences depending on the projectile parameters, a similar healing mechanism was proven. Furthermore, the importance of the presence of ionic clusters and the resulting unique properties was demonstrated by comparison with other polymers such as linear low-density polyethylene and polypropylene. In addition, certain amounts of zinc stearate (a plasticizer) were added to the ionomers, which reduced the self-healing response after several healing cycles [156]. Additionally, aliphatic di- and tricarboxylic acid-based modifiers (oxalic acid, succinic acid, adipic acid, citric acid, and sebacic acid) and the corresponding amides of sodium-neutralized analogs were added to the ionomer blend (10 wt%). In situ mechanical evaluation illustrated that only the carboxylic acid derivates reduced the elastic properties and improved the elastomeric behavior, resulting in better healing [170]. Further work from Varley and van der Zwaag pointed out that the penetration of a bullet triggers three contiguous events in the ionomer: an initial elastic response, an inelastic response, and then pseudo-brittle failure [167].

Di Landro and coworkers analyzed the self-healing behavior of ionomers blended with semicrystalline poly(vinyl alcohol-*co*-ethylene) (EVA) or epoxidized natural rubber (ENR) (15–50 wt%) [171]. In general, the addition of EVA increases the stiffness whereas ENR reduces it. Ballistic puncture tests demonstrated that addition of up to 30% EVA still results in self-healing behavior. By increasing the amount to 50% EVA, the self-healing properties are reduced, resulting in incomplete repair of the damage as a result of the higher stiffness of the film. In contrast, the ENR blends in all investigated compositions show complete self-healing behavior. The authors assigned this finding to the same or improved crystallinity of the ionomer phase [171, 172]. It was further demonstrated that EMAA ionomers

neutralized with zinc ions (10%) and afterwards mixed with ENR did not show any self-healing property as a result of several crosslinks between the epoxy group of ENR and the EMAA ionomer, which reduced the molecular mobility [173]. Recently, different epoxidation levels of ENR (25 mol% and 50 mol% ENR) were investigated in blends with EMAA ionomers in different compositions. The studies revealed that the level of epoxidation in ENR has a significant influence on the self-healing properties of the resulting blends. Only blends with 50 mol% ENR achieved self-healing [145].

Recently, Kalista et al. tested a large number of nonionic copolymers of EMAA (Nucrel 925 and Nucrel 960) and ionomers (Surlyn 8940 and Surlyn 8920) using differential scanning calorimetry (DSC), dynamic mechanical analysis (DMA), FTIR, and rheological tests [144]. The ballistic puncture was tested at temperatures ranging from −50 to 140 °C. On the basis of these data, a comprehensive self-healing "phase diagram" was created showing the healing ability as a function of the degree of neutralization and of temperature. In general, 30% neutralized EMAA provided good healing up to the order–disorder transition ($T_i = 40$ °C); 60% neutralized EMAA showed improved healing above the melting temperature ($T_m = 90$ °C). A higher amount of crosslinks, resulting from a higher amount of ionic groups, resulted in stiffer materials and thus further decreased the self-healing ability. Increasing the temperature induced mobility and, thus, self-healing was possible. A higher ionic content was suitable for healing at higher temperatures, whereas a lower ionic content was beneficial for self-healing at lower temperatures. These findings suggest that hydrogen bonds additionally act as reversible crosslinks at low temperatures, whereas ionic clusters are the responsible reversible crosslinks at elevated temperatures.

Furthermore, the two-stage mechanism was extended by a subsequent third stage: the long-term reorganization of polymer chains, resulting in a stable polymer structure [144, 146]. To learn more about the last two stages of the mechanism, acoustic and ultrasonic time-dependent resonant spectroscopy (TSRS) was performed by Ricci and coworkers [174]. Two ionomers based on EMAA were measured from 1 kHz to 2 MHz before and after damage. This method facilitates the investigation of energy dissipation, relaxation, and morphology of self-healing ionomers. After the damage occurred, the self-healing process began immediately. During the second stage, the material is welded and finally sealed. Long after these visible events, TSRS proved the presence of quality factor variations in the resonance spectra resulting from energy dissipation instability (Surlyn 9840 7 h; Surlyn 9820 >18 h), which were ascribed to long-term reorganization within the polymer.

To evaluate ionomers for application in astronautics, hypervelocity ballistic tests of Surlyn 9840 were performed [175]. It was demonstrated that complete healing of 5-mm thick ionomer films damaged by impact at velocities of 2–4 km/s is possible. Furthermore, the self-healing ionomer was compared with thin-wall aluminum-alloy bumpers (AL-7075-T6) [176]. In general, the ionomers showed lower primary damage than aluminum. However, it was found that aluminum bumpers have better debris fragmentation abilities than ionomers. Furthermore, Sundaresan et al. demonstrated the healing ability of a composite material based on EMAA

and carbon fibers after medium-velocity impact and proposed their utilization for aerospace applications [177].

4.2 Self-Healing of Ionomers After Nonballistic Impact

As an alternative to ballistic high-energy impact puncture and instantaneous starting of the self-healing process, a handful of studies have reported self-healing based on different polymer structures or different testing procedures. Maure et al. generated a two-component system that included particles or fibers of an EMAA copolymer (Nucrel 2940) and carbon fiber laminates [178]. The melt of EMAA generated after heating to 150 °C for 30 min is able to flow into the damage zone and can act as the healing agent. Therefore, fractured surfaces were re-bound and initial properties were almost completely restored after heating. The same phenomenon was observed in systems made by adding EMAA to epoxy resins [179]. Furthermore, Pingkarawat et al. added EMAA copolymers to carbon fiber-epoxy laminates to investigate their influence on the material properties and self-repair capacity [180, 181]. On the one hand, the addition of EMAA improved the ability to heal delamination cracks after thermal treatment. On the other hand, the original toughness of the laminates was optimized.

James et al. designed a system (EMAA neutralized with zinc) in which the ionomer was utilized to restore piezoelectric properties [143]. For this purpose, zirconium titanate powder was dispersed within the ionomer. After the damage event, the mechanical properties and the lost piezoelectric properties could be repaired by thermal healing. Magnetically activated healing of ionomeric elastomers was recently investigated [182]. The self-healing effect was achieved by heat dissipation of the introduced magnetic nanoparticles and was studied with the help of tensile experiments. Almost full repair of the tensile strength after 10 min was possible using electromagnetic treatment. The material is potentially utilizable in hard-to-reach areas, because of the fast response and the non-contact healing properties of the system.

Mecerreyes and coworkers reported a new class of supramolecular ionic polymers based on compounds with multiple carboxyl or amine functions [183]. Rheological tests demonstrated a transition of the formed gel into a viscous liquid between 30 °C and 80 °C. Initial self-healing tests showed the ability of this material class to self-heal scratches on the surface or to re-bind two separated pieces during low energy impact. Furthermore, an ionic network formed by the combination of citric acid and different aliphatic diamines provided a network with unique rheological properties, which featured good self-healing potential [184]. Recently, the authors also expanded the new polymer class with various chemicals from renewable sources [185].

Bose et al. investigated an ionomeric elastomer with respect to the content of ionic groups and the influence of the utilized counterion [142]. The authors synthesized poly(butyl acrylate-*co*-acrylic acid)s with different compositions.

Neutralization with sodium, zinc, and cobalt resulted in a range of different ionomers. These materials were studied with temperature-dependent dynamic rheology combined with simultaneous FTIR analysis. An important parameter, supramolecular bond life (τ_b) (i.e. the time required for cleavage and re-bonding of reversible bonds), was thought to enclose the required parameters (i.e. dynamic character of the reversible interactions) for scratch healing, leading to a correlation between these two factors. A supramolecular bond life of 10–100 s is ideal to enable enough mobility of the polymer chains for ideal macroscopic healing. Recently, the same polymer architecture was utilized to investigate the influence of different amounts of cobalt salts (3, 5, and 7% cobalt) [186]. In this context, chain dynamics and relaxation lifetimes were calculated and compared with the macroscopic self-healing behavior of the cobalt ionomers. It was pointed out that the cluster activation determines the healing kinetics.

Although the EMAA copolymer and its ionomers have been well investigated, other ionomeric polymer classes receive less interest. New methods, such as ^{1}H low-field NMR measurements [187], for investigating self-healing ionomers with respect to their mechanical and self-healing behavior should yield a more detailed understanding of the mechanism. These results could provide evidence for structural changes in the polymer itself, which result in improved properties of the resulting material. Another strategy is to mimic processes found in nature, such as the self-healing achieved in human bones [188].

5 Self-Healing Metallopolymers

Compared with ionomers, which exhibit cluster formation of the ionic groups, the reversible character of metallopolymers can have a different origin. Besides the reversible non-covalent metal–ligand interactions, metallopolymers can also benefit from clusters generated from the metal ions and the corresponding counterion or simply as a result of phase separation [189]. Thus, metal–ligand interactions as crosslinks can imbue polymers with tunable mechanical and self-healing properties. An overview of the state of the art in metallopolymers is presented in Table 2.

In 2005, Varghese et al. demonstrated a self-healing hydrogel based on acryloyl-6-amino caproic acid (A6ACA) after treatment with a copper(II) chloride solution at ambient temperature [208]. After 12 h, 75% of the tensile strength was recovered. If the gel was added to an aqueous solution without the metal salt, no self-healing behavior was observed. This indicates that the self-healing process was mediated by the metal ions. Another metallogel was presented by Chen and coworkers [196]. The authors synthesized 2,6-bis(1,2,3-triazole-4-yl)pyridine (BTP)-containing polyurethanes via the copper(I)-catalyzed azide–alkyne 1,3-dipolar cycloaddition (CuAAC). The ligand BTP is incorporated in the polymer backbone and can be crosslinked with Zn^{2+}, Ni^{2+}, Fe^{2+}, and Ru^{2+} in a stoichiometry of 1:2 (metal to ligand). Furthermore, crosslinking with Eu^{3+} leads to 1:3 complexes. Gels

Table 2 Summary of ligand–metal systems utilized for the design of self-healing metallopolymer networks

Ligand system	Metal	References
Catechol	Fe^{3+}	[190, 191]
Histidine	Zn^{2+}	[192, 193]
	Ni^{2+}, Co^{2+}, Cu^{2+}	[192]
Imidazole	Zn^{2+}	[194]
Poly(ethyleneimine)	Cu^{2+}	[195]
Pyridine		
2,6-Bis(1,2,3-triazole-4-yl)pyridine (BTP)	Zn^{2+}, Eu^{3+}	[196–198]
	Tb^{3+}	[198]
2,6-Bis(1′-methylbenzimidazolyl)pyridine (Mebip)	Zn^{2+}, La^{3+}	[199]
4,4′-{[(Pyridine-2,6-dicarbonyl)bis-(azanediyl)]bis(methylene)}-dibenzoic acid	Eu^{3+}, Tb^{3+}	[200]
4-(Pyridin-2-yl)-1*H*-1,2,3-triazole	Fe^{2+}, Co^{2+}	[201]
Terpyridine	Ni^{2+}	[202]
	Fe^{2+}	[203, 204]
	Cd^{2+}	[205]
Tyrosine	Ni^{2+}	[206]
L-Valine	Zn^{2+}	[207]

swollen in acetonitrile or THF and crosslinked with $Zn(OTf)_2$ or $Eu(OTf)_3$ demonstrated excellent self-healing behavior. Another approach using CuAAC to copolymerize BIP and spiropyran (SP) in a polyurethane backbone was shown [197]. The addition of Zn^{2+} or Eu^{3+} leads to the formation of supramolecular gels revealing a hard/soft morphology. Zinc-containing gels showed better self-healing properties compared with Eu^{3+}. Recovery of the original mechanical properties after treatment with solvent was achieved. Recently, Yang et al. synthesized BIP-containing polymers via thiol–ene "click" reactions [198]. The corresponding gel was formed by mixing with Zn^{2+}, Eu^{3+}, or Tb^{3+} salts. Rheological analyses of the three gels demonstrated that the storage modulus G' fully recovers after damage within 20 min. Terech et al. utilized bis-terpyridine cyclam as tritopic ligand for nickel ions, resulting in a supramolecular gel [202]. In addition, a fatty acid organogel based on 12-hydroxy stearic acid (HSA) with similar elasticity was utilized to compare the self-healing properties. First, the different gels were damaged with a spatula in a test tube, which was then placed upside down. In contrast to the HSA gel, the metallogel revealed a recovery of the strain after 48 h. The metallo-supramolecular gel showed a recovery capability of up to 72%, whereas the HSA gel exhibited only 32%.

Multistimuli-responsive healable hydrogels based on nickel–tyrosine interactions were described by Banerjee and coworkers [206]. Interestingly, TEM studies indicated nanofibers in the range of 60–150 nm. All hydrogels healed within 30 min of putting the cut pieces together. Rheological experiments also showed the recovery of up to 83% of their original stiffness. The variation in chain length of the

tyrosine derivates influences the self-healing ability (i.e., longer chain length correlates with faster self-healing). Additionally, the same group investigated the self-healing properties of a non-polymeric supramolecular hydrogel based on an L-valine-functionalized ligand and Zn^{2+} ions [207]. In addition to interesting multiresponsive gel-to-sol and sol-to-gel transitions, the hydrogel can bear 60-fold its own weight without any change in shape. Furthermore, it exhibits rapid self-healing behavior at room temperature. Recently, a pyridine-2,6-dicarboxylic acid derivate was utilized to design self-healing luminescent supramolecular metallogels [200]. For this purpose, lanthanides (i.e., Eu^{3+} and Tb^{3+}) were added in different stoichiometric ratios. The nature of the metal salt influences the resulting color. The metallogels were further swollen in methanol to enable self-healing of these materials. Gels with only one metal ion show instantaneous self-healing after cutting the material. Rheological studies showed that the gel containing both Eu^{3+} and Tb^{3+} is softer than gels with only Eu^{3+} or Tb^{3+}. However, all gels provide fast recovery of the initial G' after damage.

The first photoinduced self-healing of a metallopolymer was reported in 2011 [199]. Here, Burnworth et al. end-functionalized poly(ethylene-*co*-butylene) with two 2,6-bis(1′-methylbenzimidazolyl)pyridine (Mebip) ligands. The addition of $Zn(NTf_2)_2$ or $La(NTf_2)_3$ leads to linear metallopolymers that showed self-healing under irradiation with UV light (320–390 nm, 950 mW/cm^2). The irradiation induced two different phenomena: Cleavage of the metal–ligand complex and heating of the polymer (approximately 220 °C). Consequently, the flexibility of the polymer increased, which enabled healing. After irradiation, both metallopolymers can rapidly recover their initial mechanical properties (~1 min). Wang et al. copolymerized *n*BA and methyl methacrylate with a Mebip-containing acrylate via RAFT polymerization (approx. 3, 5, or 8% Mebip) [209]. Subsequent crosslinking with $Zn(OTf)_2$ led to a gel, whereas crosslinking with $Eu(OTf)_3$ resulted in a highly viscous material. This fact indicated that Eu^{3+} binds more weakly than Zn^{2+} to Mebip. Rheological measurements further revealed that the amount of crosslinks influenced the storage modulus (G'). Thus, a higher Mebip content, corresponding to a higher crosslinking density, led to higher G'. Furthermore, T_g increased with a higher content of Zn^{2+} and, similarly, the viscous flow temperature (T_f) increased. The material showed both shape-memory and healing properties. For self-healing tests, a copolymer containing 5% of Mebip was used because of its good mechanical properties. First, a rectangular plate of this material was damaged with a razor blade and then the plate was bent at an angle of 90° to separate the crack surfaces. Heating to 140 °C initiated a shape-memory-assisted self-healing process (SMASH) and healing was obtained within 25 min. Furthermore, the healing ability during irradiation with UV light (300–400 nm, 127 mW/cm^2) was investigated. Here, the polymer was heated to 185 °C, which enabled healing within 4 min.

Recently, Wang and Urban presented a supramolecular network based on copper–poly(ethyleneimine) (PEI) interactions. The resulting metallopolymer was capable of healing under irradiation with UV light [195]. The key step for the healing process is not the heating of the polymer network during UV irradiation, but

the UV-induced re-formation of the Cu-amine complexes. UV absorption induces a square-planar-to-tetrahedral transition of the Cu-PEI complex. The ground state of the Cu-amine complex has a square-planar geometry as a result of the high energy difference between $d_{x2-y2}$and $d_{xz/yz}$ orbitals. After UV irradiation, the energy difference between these two orbitals is decreased, which leads to transition to the tetrahedral structure. In the self-healing experiments, the material was completely cut into different pieces. The combined pieces healed multiple times under UV light. Furthermore, films of this network were coated onto a glass substrate and mechanically damaged. Surprisingly, the self-healing process was only possible two to three times.

Bode et al. synthesized terpyridine-functionalized poly(alkyl methacrylates) via the RAFT polymerization technique [203]. The polymers containing approximately 10% terpyridine units were crosslinked by the addition of iron(II) sulfate. The authors utilized methyl-, butyl-, and lauryl methacrylate as comonomers for the copolymerization. Thus, different T_g values were observed, decreasing with longer side chains. Therefore, no self-healing behavior of the poly(methyl methacrylate)-based polymer was observed as a result of the high T_g of 74 °C. In the other two cases, self-healing was achieved at 100 °C. Films based on butyl methacrylate revealed the healing of small cracks (length 180 μm, width 10 μm) within 40 min of damaging the film with a scalpel. However, reducing the temperature to 80 °C led to a significantly longer healing time (i.e. 30 h). Changing the comonomer to lauryl methacrylate resulted in a more flexible network. Consequently, the polymer film healed larger and wider scratches. Moreover, SAXS measurements of the metallopolymer suggested the presence of (ionic) clusters. Temperature-dependent Raman spectroscopy indicated that free terpyridine moieties are present during healing as a result of partial thermal decomplexation. In addition, quantum mechanical/molecular mechanical (QM/MM) simulations were performed to investige two possible healing mechanisms: (1) Thermal decomplexation of the metal–ligand interaction and the formation of new crosslinks upon cooling and (2) thermal dissociation of the ionic clusters (Fig. 17). The possibility of thermal decomplexation was confirmed by QM/MM simulations. In contrast, these simulations revealed that neither complete thermal cleavage of the relatively stable ionic cluster nor formation of new crosslinks are possible at the applied temperature (100 °C) [204].

Further investigations revealed that the self-healing behavior is connected with the strength of the metal–ligand interaction. As a consequence, variation of ligands and metal salts are key factors in tuning these intrinsic properties [189]. In the same manner, the self-healing behavior of terpyridine-containing polymers was improved by changing the metal ion as well as the counterion. Cadmium acetate was utilized as the crosslinker, because of weaker metal–ligand interactions (compared with iron). The resulting materials showed multiple healing cycles at 80 °C [205]. Furthermore, the formation of monoterpyridine complexes was verified, which are crosslinked via acetate bridges. Recently, an alternative ligand system was utilized to design self-healing materials [201]. A bidentate triazole-pyridine was copolymerized with lauryl methacrylate via RAFT. Crosslinking with iron

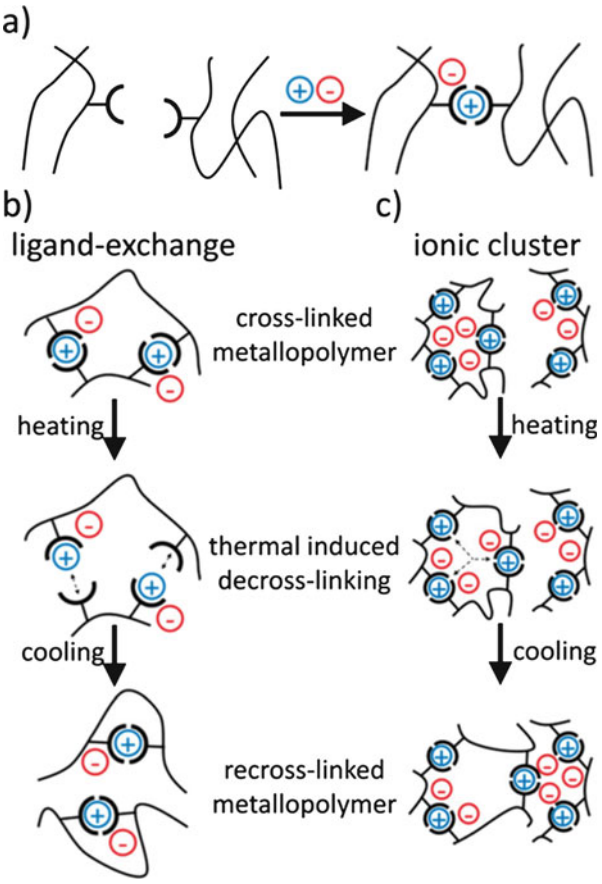

Fig. 17 Proposed healing mechanism of metallopolymers: (**a**) crosslinking by the addition of a metal salt, (**b**) reversibility based on ligand-exchange, and (**c**) reversibility based on ionic cluster (reprinted with permission from [204])

(II) and cobalt(II) salts led to self-healing polymers that could heal at temperatures between 50 and 100 °C.

Further investigation of this system also revealed a correlation between the supramolecular bond lifetime and the healing behavior of metallopolymers [210]. For this purpose, a terpyridine-containing poly(butyl methacrylate) was crosslinked by the addition of 12 different metal salts. Manganese(II), cobalt(II), zinc(II), and nickel(II) were chosen as cations and chloride, nitrate, and acetate as the corresponding anions. The healing behavior of these 12 metallopolymers was investigated. The polymer network crosslinked by manganese(II) chloride featured the best self-healing behavior. The mechanical properties were studied by rheology and a crossover of G' and G'' was demonstrated, which is related to the self-healing behavior of the metallopolymer.

Guan and coworkers designed a multiphase network consisting of zinc–imidazole interactions in a hard/soft brush copolymer structure [194]. First, they copolymerized styrene and 4-vinylbenzyl chloride (5 and 10%) via free radical polymerization (approximately 140 repeating units). Post-polymerization

functionalization of the benzyl chloride with potassium ethyl trithiocarbonate enabled selective introduction of a RAFT chain transfer agent. Subsequently, the trithiocarbonate was utilized for the RAFT polymerization of *n*BA with an imidazole-containing acrylate (approximately 180 repeating units). The imidazole content was adjusted to 25 or 35 mol%. SAXS measurements revealed the presence of a broad reflection corresponding to a domain size of 7–20 nm. Furthermore, the mechanical properties were tuned by varying several polymer parameters (e.g., the content of imidazole and the ratio between ligand and zinc salt). Self-healing tests were performed by cutting the material to a depth of 70–90% of the material thickness. Afterwards, the material was reconnected for 1 min at room temperature. Recovery of the original mechanical properties was analyzed in a tensile test, which revealed full recovery of the toughness after 3 h. Interestingly, the Young's modulus and the yield stress recovered rapidly.

Scientists are often inspired by nature. On the one hand, macroscopic self-healing in nature can rehabilitate broken bones or injured skin and, on the other hand, it can occur on a molecular scale. Repair of DNA through various processes after self-replication [211], regeneration of hydra (fresh-water polyps) [212], recovery of egg capsules of marine whelks [213], and the self-healing behavior of mussel byssal threads after stress [214] are just a few of thousands of natural examples. However, the latter example has been widely discussed in recent years [215–220]. The material exhibits both the interaction between 3,4-hydroxy-phenylalanine (DOPA) and iron ions [190, 221] and histidine–metal interactions [217, 222]. In detail, mussel byssus consists of several threads and acts as a shock-absorbing line for mussels in marine environments. Secreted by the mussel foot, the threads attach the organism to rocks with an adhesive plaque built-up from several DOPA-containing proteins. Furthermore, the mussel thread consists of a distal and a proximal region. It was found that the self-healing behavior might be based on histidine–zinc interactions in a block copolymer-like protein structure [214, 218, 220, 223].

The first study by Holten-Andersen et al. utilized catechol-Fe^{3+} and its pH dependency to form self-healing polymer gels [190]. DOPA-containing star-shaped branched poly(ethylene glycol) (PEG) chains were synthesized and further crosslinked with iron(III) chloride. Deprotonation of the hydroxyl groups of DOPA leads to a variation in the stoichiometry of the DOPA-Fe^{3+} complexes (Scheme 2). The changes in the complex structure can be monitored by UV–vis spectroscopy, which verified the pH values of ~5, ~8, and ~12 for the mono-, di- and tris-complexes, respectively. Furthermore, resonance Raman spectroscopy of the hydrogel at high pH values corresponds to results obtained from native mussel thread cuticles. Self-healing tests demonstrate almost full recovery of stiffness and cohesiveness after damage.

This system was recently investigated with respect to tenability via control of crosslinking by variation of the metal ions [191]. For this propose, chloride salts of iron(III), vanadium(III), and aluminum(III) were added in a ratio of 1:3 (metal to catechol). The pH was adjusted to 8 to mimic typical oceanic conditions. UV–vis spectroscopy showed that the vanadium-based gels exhibit tris-catechol complexes

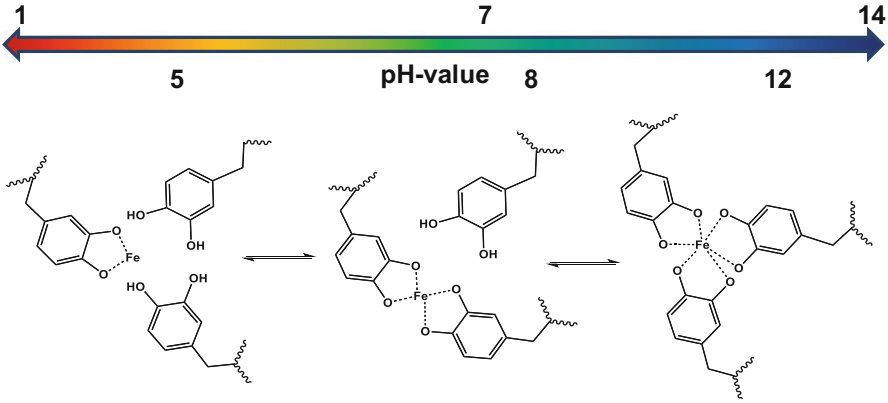

Scheme 2 Complexes of iron(III) ions with catechol and their pH-induced crosslinking character

and that di-catechol complexes were obtained using iron-based gels. In contrast, the aluminum–catechol interactions were thought to be the weakest, because of the low UV–vis-absorption of the polymer gel. Resonance Raman spectroscopy measurements supported these results. Therefore, vanadium is an optimal coordination partner for DOPA-based polymer gels at pH 8. Results showed a tenfold higher stability of the gel containing vanadium compared with the iron-based system. These findings illustrate the dependency of the complex structure on both pH and metal salt. This study provides excellent inspiration for new self-healing materials. In addition, Krogsgaard et al. utilized DOPA-containing polyallylamine, crosslinked with $FeCl_3$, to further optimize the self-healing behavior of such hydrogels [224]. After damaging this hydrogel with a spatula at pH 8, full recovery of the original shape and mechanical strength was achieved. Tensile tests also confirmed a fast recovery of the storage modulus G' of 4,700 Pa.

Another mussel-inspired approach is the utilization of metal–histidine interactions for formation of self-healing materials. Fullenkamp et al. studied a four-arm star polymer based on terminal-functional histidine-modified PEG [192]. This polymer was subsequently crosslinked with zinc(II), copper(II), nickel(II), and cobalt(II) ions in a ratio of 1:2 and 1:4 (metal to histidine). The resulting hydrogels were investigated via rheology. The authors reported that the rate of self-repair follows the order $Zn^{2+} > Cu^{2+} > Co^{2+} > Ni^{2+}$. Recently, Enke et al. developed for the first time self-healable coatings based on zinc–histidine interactions [193]. For this purpose, two novel histidine monomers were synthesized. Both histidine moieties were protected with a triphenylmethyl group (Trt) on the N^{τ}-position to optimize their solubility in organic solvents. In the case of the first monomer (Trt-His-OMe, **1**), the acid function is blocked with a methyl ester, whereas the second monomer (Trt-His-OH, **2**) bears free carboxylic acid (Fig. 18).

Afterwards, butyl methacrylate (BMA) and lauryl methacrylate (LMA) were copolymerized with those histidine monomers via RAFT polymerization. In a further step, the Trt group was cleaved off in order to visualize the influence of

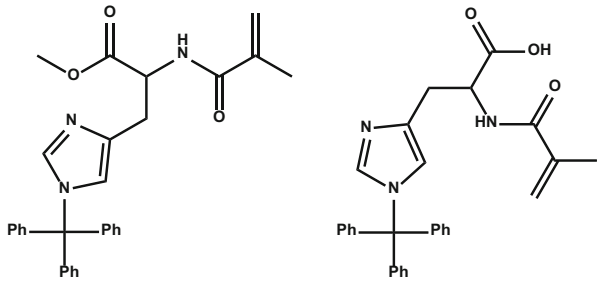

Fig. 18 Novel histidine monomers **1** and **2**

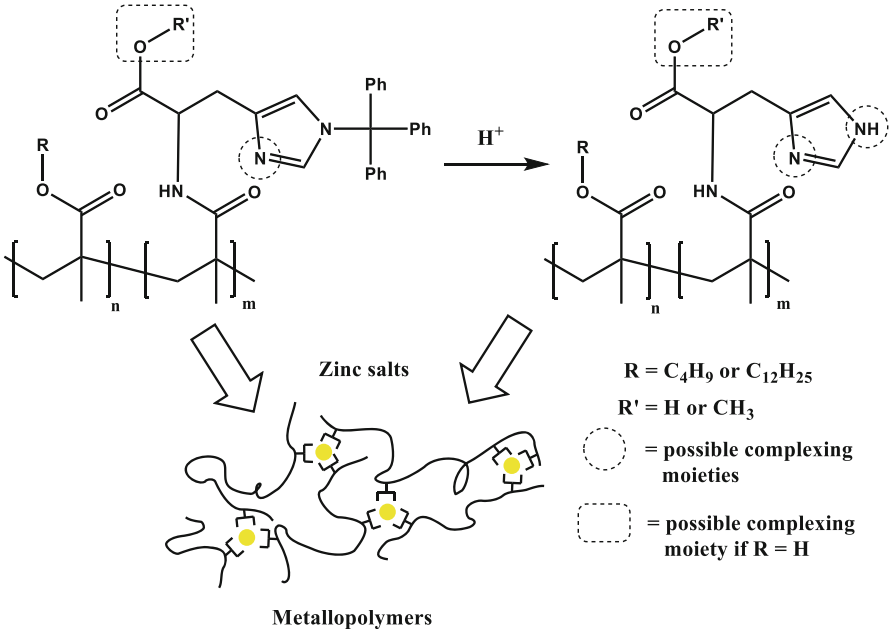

Scheme 3 Histidine monomers and synthesis of the corresponding copolymers, which were further crosslinked with several zinc salts (reproduced with permission from [193])

the protecting group (Scheme 3). Finally, the different copolymers were crosslinked with several zinc salts in the ratio 1:3 (zinc to histidine) and drop-coated onto microscope slides. The resulting films were investigated with respect to their crack-healing behavior. Best self-healing results were found for LMA/**1**-containing metallopolymers (40–60 °C within 20 min). In general, LMA copolymers demonstrate better self-healing as a result of their longer side chain, which mediates higher flexibility. Furthermore, the counterion is found to have a considerable influence on the self-healing capacity. Thus, the utilization of zinc(II) nitrate results in the best

self-healing properties compared with zinc(II) chloride and zinc(II) acetate. This fact leads to the suggestion that the binding strength of the counterion is responsible for this behavior. Cleavage of the Trt group of Trt-His-OMe-containing metallopolymers leads to an increase in the temperature required for the self-healing process. The higher binding strength of the formed complexes as a result of the higher coordination possibilities might require more energy to show reversibility. Another trend was found in the case of Trt-His-OH-containing copolymers. Here, the self-healing temperature significantly decreased after cleavage of the Trt group. The authors supposed that the free carboxylic acid function plays a key role in the structure of the histidine–zinc complexes, which influences the self-healing behavior extensively. However, this effect should be further investigated in detail to obtain the required information for enhancing self-healing behavior in a controlled manner.

In recent years, promising strategies for self-healing metallopolymers have been developed and further improved. A deeper understanding of the self-healing mechanism for each metal–ligand system is a key factor in designing well-defined future self-healing materials. Furthermore, the processability of the metallopolymers, in particular of the networks, has to be improved to enable broader applications.

6 Self-Healing Polymers Based on Reversible Host–Guest Interactions

Compared with metal–ligand interactions, the non-covalent binding between a host and a guest (i.e. molecular recognition) can be based on several interactions, such as van der Waals, charge-transfer, ion-dipole, and hydrophobic interactions [225]. A typical example of a host–guest interaction is the human immune system with its antibodies, which selectively bind on antigens and finally eliminate pathogens. Furthermore, enzymes are known for their catalytic influence via selective reactions (i.e. key and lock model) [226].

Self-healing supramolecular networks based on host–guest interactions are a relatively new topic, begun with the pioneering work of Harada and coworkers in 2011 [227]. Since then, several macrocyclic hosts (cyclodextrins, crown ethers, and cucurbit[*n*]urils) have been used for the preparation of self-healing supramolecular networks (Fig. 19).

Cyclodextrins (CDs) are water-soluble macrocycles consisting of six, seven, or eight to 16 glucose units linked by α-1,4-glycosidic bonds. Most utilized cyclodextrins are α-, β- and γ-CDs consisting of six, seven, or eight linked units [228, 229]. Moreover, the possibility of synthesizing polymers containing CDs via controlled radical polymerizations (e.g., RAFT) or post-polymerization functionalization offers easy synthetic pathways [230]. The CDs can form inclusion complexes with a large number of guests through hydrophobic interactions.

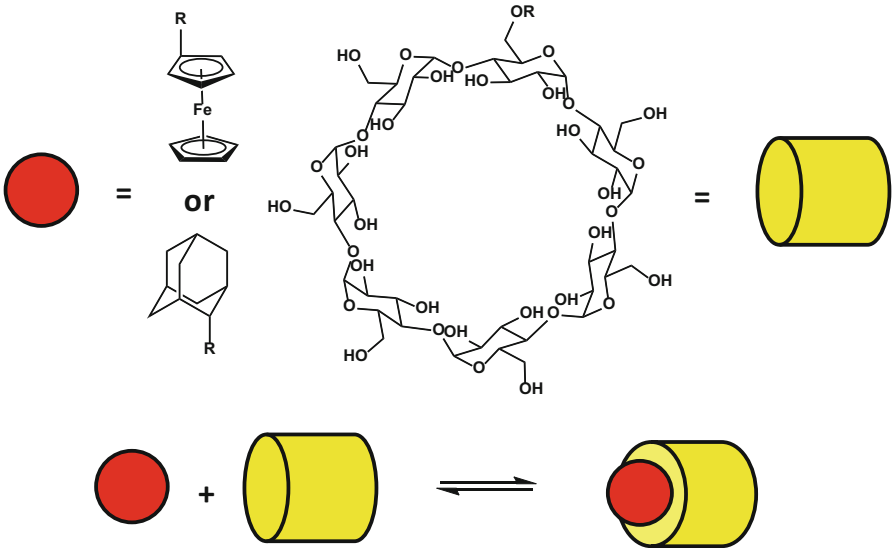

Fig. 19 Host β-cyclodextrin with ferrocene and adamantane as guest molecules with a binding stoichiometry of 1:1

Important guests for self-healing materials are ferrocene and adamantane units (Fig. 19) [231].

The unique reversibility of the host–guest interaction between β-CD and ferrocene (Fc) was utilized by Harada and coworkers to design the first example of those materials [227]. For this purpose, poly(acrylic acid) was functionalized with either β-CD or Fc. The two functionalized polymers were mixed together to form a supramolecular hydrogel. The authors utilized the redox-responsive host–guest interaction to induce a sol–gel phase transition of the hydrogel. β-CD has a high affinity for the neutral Fc; however, the complex rapidly dissociates when Fc is oxidized (Fc^+) [232]. The self-healing properties were also investigated. When the material was cut into two pieces and, subsequently, brought into close contact, the two halves reconnected within 24 h. The adhesive strength of the material was recovered up to 84% of the initial strength. To demonstrate the dependency of the self-healing process on the reversible host–guest interactions, the freshly cut surface was treated with competitive guest and host molecules. After 24 h, the connected pieces showed no self-healing. In addition, the influence of an oxidizing reagent was studied with respect to control of the self-healing ability. The addition of an aqueous solution of sodium hypochlorite to the freshly cut surface resulted in oxidation of Fc to Fc^+, which led to no complex formation with β-CD. Hence, self-healing was not obtained. The authors discussed the potential utilization of these materials for drug delivery because of their excellent properties and the biocompatibility of cyclodextrin.

Yan et al. synthesized a water-soluble oligo(ethylene glycol) (OEG) functionalized with ferrocene (Fc-OEG-Fc) and cyclodextrin (β-CD-OEG-β-CD) units [233]. By mixing these monomers together an AA–BB-type supramolecular polymerization was achieved. Furthermore, these polymers showed hierarchical assembly into nanofibers and self-degradable and self-healing properties under electrochemical conditions.

Self-healing polymers triggered by electrochemical stimuli, based on poly (glycidyl methacrylate) modified with Fc and difunctional β-CD, were fabricated [234]. The self-healing properties of the coated polymer films were investigated with scanning electron microscopy (SEM). The best self-healing behavior was obtained by electrical treatment with a 9-V cell for 24 h and subsequent heating to 85 °C for 24 h. In addition, utilization of the polymer as a self-healing agent in commercial painting products was tested successfully.

Wang et al. utilized fatty acids modified with β-CD and poly(ethylenimine) oligomer-grafted Fc, in the design of a supramolecular network with self-healing properties [235]. After cutting this material into pieces and then bringing the pieces together, the material healed within 5 min (the presence of absorbed water is required for self-healing). To determine the importance of the host–guest interaction on the healing process, competitive hosts were added onto the freshly cut surfaces and resulted in no self-healing even after 24 h. Therefore, the interaction between the host and the guest plays a key role in the self-healing mechanism. The authors address the possibility of utilizing the presented system as an efficient cushioning material. Recently, β-CD and Fc were separately introduced as pendant groups in a poly(*N*,*N*′-dimethylacrylamide) backbone. The resulting hydrogel was formed by simple mixing of the two polymers in an aqueous solution. Self-healing was proven by rheological tests; damaged hydrogels could rapidly restore their initial level. In addition, cytotoxicity measurements demonstrated the biocompatibility of these materials, enabling biological applications such as tissue engineering and drug delivery [236].

Another important guest for cyclodextrin-based self-healing systems is adamantane (Ad). Harada and coworkers presented the formation of a hydrogel by copolymerization of acrylamide and the inclusion complex of a CD monomer with the guest monomers *n*BA or *N*-adamantane-1-yl-acrylamide in water [237]. After cutting the β-CD-Ad hydrogel into half and then putting the surfaces together, the surfaces more or less immediately formed one piece again. In contrast, the rejoined two pieces of the α-CD-*n*BA hydrogel required several hours to achieve reattached material. Complete recovery of the gel strength of β-CD-Ad hydrogel took 24 h, whereas the α-CD-*n*BA hydrogel restored only 74% of the initial strength after the same time. The different behavior of the hydrogels is associated with the higher binding constant of β-CD with an Ad group ($K_a = 1{,}500\ M^{-1}$) than α-CD with *n*BA ($K_a = 57\ M^{-1}$). In addition, self-healing of the β-CD-Ad hydrogel was achieved even if the two halves were separately stored for 20 h and brought together afterwards. Recently, Harada and coworkers demonstrated a hard self-healing xerogel based on host–guest interactions of β-CD and Ad [238]. For self-healing tests, the β-CD xerogel and the Ad xerogel were

mixed together. The molar ratio (mol%) of the host and the guest was varied. The self-healing capacity of β-CD-Ad xerogels was investigated by tensile tests. The xerogel containing 0.3 mol% of β-CD and 0.4 mol% of Ad showed an adhesive strength of 2.8 MPa. After damage, the reattached xerogel demonstrated a recovery stress ratio of 40% after 1 h and 88% after 48 h.

Himmelein et al. prepared an Ad-modified cellulose polymer that was crosslinked with cyclodextrin-containing vesicles [239]. This material revealed shear-thinning and self-healing properties. Recently, Zhang et al. presented a self-healing conductive network based on small molecules and nanotubes [240]. The authors utilized single-walled carbon nanotubes containing β-CD and Ad-modified PEI to fabricate a recyclable supramolecular composite. The material restored its initial electrical and mechanical properties to over 90% after damage (tensile tests). Nevertheless, the addition of water is required for the self-healing process. The authors proposed that the self-healing is based on host–guest interactions as well as on hydrogen bonds. Rodell et al. modified hyaluronic acid separately with β-CD and Ad [241]. The Ad unit is bound to the polymer backbone via a peptide chain, which offers the possibility of proteolytic degradation of the network. After mixing these polymers, a hydrogel with self-healing behavior is formed. The authors highlighted the injectability and the biodegradability of the presented material with the potential for medical applications such as drug or cell delivery.

Zhu and coworkers synthesized a photoresponsive supramolecular hyperbranched polymer based on the non-covalent interactions between an azobenzene dimer and a β-CD trimer [242]. The authors suggested further investigation of its self-healing properties because of the photocontrolled reversible complexation of the host by the guest by alternating UV–vis irradiation. This principle is based on the different aggregation constant between β-CD and either the *trans*- or the *cis*-isomer. Selective irradiation with 365 nm led to the *cis*-conformation, which has a much lower association constant with β-CD than the *trans*-isomer, resulting in dissociation of the polymer. This effect generated mobility in the material and enabled healing (e.g., crack healing in a coated polymer film). Chen et al. investigated the host–guest interactions between β-CD and α-bromonaphthalene (α-BrNp) in a hydrogel based on a polyacrylamide backbone [243]. After cutting the material into pieces and placing the surfaces together, rapid self-healing behavior was observed (1 min). The rheological properties were restored after 1 h. The authors pointed out that the self-healing behavior is influenced by both host–guest interactions as well as hydrogen bonds. In addition to the self-healing properties, the hydrogel showed the ability to produce room-temperature phosphorescence.

Yu et al. utilized a new method for radical polymerization (magnetically induced frontal polymerization, MIFP) to synthesize Fe_3O_4-doped supramolecular gels based on the host–guest recognition of β-CD and *N*-vinyl imidazole (VI) copolymerized with 2-hydroxypropyl acrylate [244]. Thus, the β-CD moiety is not included in the polymer chain. The ability of VI to form dimer inclusion complexes with β-CD enables reversible crosslinks in the polymer matrix. Increasing the amount of β-CD and introduction of Fe_3O_4 nanoparticles significantly

improved the mechanical properties. However, increasing the β-CD concentration can block the imidazole groups, resulting in a decreased self-healing capacity. A β-CD to VI ratio of 1:5 (w/w) was found to represent an optimum between mechanical and self-healing properties. Furthermore, the healing time was significantly decreased when the damaged gels were treated with an external magnetic field of 450 kHz.

Compared with cyclodextrin, which mainly forms host–guest interactions in aqueous solutions, organic solvents are utilized for crown ether-based supramolecular polymers [245]. Crown ethers have a long history, beginning with the discovery of these cyclic polyethers in 1967 [246]. They can be utilized for the complexation of metals or organic ions. Moreover, the host–guest recognition is responsive to temperature, pH, and competing ions. These properties can be utilized to introduce self-healing behavior in crown ether-based polymers [231]. In 2012, Huang and coworkers presented the first self-healing supramolecular gel with crown ether moieties [247]. For this purpose, poly(methyl methacrylate) containing dibenzo[24]crown-8 (DB24C8) was synthesized and crosslinked with two bis-(ammonium salts) having different end-group sizes (Fig. 20). Gel **1** was immediately prepared by simple mixing of the two compounds in organic solvents. Gel **2** was formed by heating for 30 days and stirring for further 45 days after mixing. The longer time for recognition is explained by the larger size of the end group (cyclohexyl unit). The host–guest interactions were proven by ^{1}H NMR

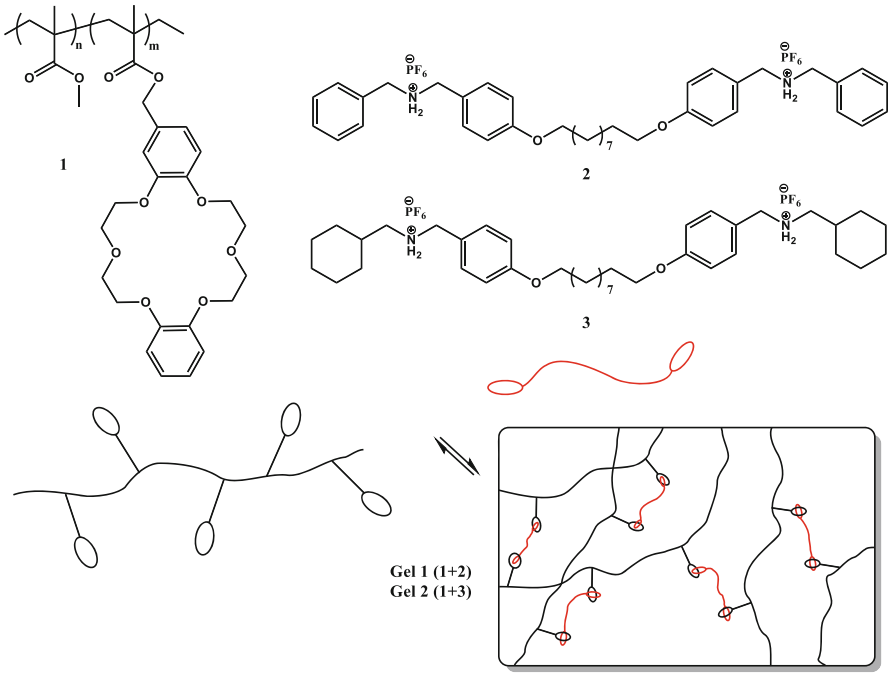

Fig. 20 Supramolecular gels based on crown ether interactions [247]

spectroscopy, indicating a chemical shift for the aromatic protons after complexation. Moreover, the gels are degradable, triggered by pH stimuli; for example, addition of a base causes deprotonation of the amines, resulting in disintegration of host and guest. Self-healing studies pointed out that the self-healing mechanism of gel **1** is based on host–guest interactions, whereas gel **2** can heal mainly through electrostatic interactions and hydrogen bonds, resulting in faster self-healing behavior. Furthermore Chen and coworkers investigated the host–guest interactions of DB24C8 and dibenzylammonium (DBA) [248]. The supramolecular network was based on a triptycene-based bis(crown ether) and a copolymer containing DBA. The resulting gel showed thermo-, acid/base- and chemo-induced gel–sol transitions. Furthermore, self-healing behavior was demonstrated after damaging the gel with a knife. The copolymerization of ethyl acrylate and a guest monomer containing DBA led to another supramolecular network if a DB24C8-containing bis(crown ether) was utilized for crosslinking [249]. The gel showed pH- and thermoresponsive behavior. Moreover, a mechanical strength of 14.8 kPa and fast self-healing properties distinguished the material.

A self-healing supramolecular organogel based on the crosslinks of DB24C8 and DBA, which were separately incorporated in a glycidyl triazole polymer backbone, was described by Ikeda and coworkers [250]. The advantage of this gel is the high elasticity under large deformation as a result of the mobile polymer chains with higher molar masses.

Huang and coworkers prepared novel crosslinked supramolecular networks based on a linear polymer: AA monomer bis(benzo-21-crown-7) (B21C7) and BB monomer bis(dialkylammonium salt) [251]. Additional 1,2,3-triazole groups were crosslinked with $PdCl_2(PhCN)_2$, resulting in a highly crosslinked, transparent self-healable gel, which also showed quadruple-stimuli responsive gel–sol transitions. The combination of two reversible non-covalent bonds led to a supramolecular polymer network with unique properties. In this way, good mechanical properties were introduced with the formation of relatively strong metal–ligand interactions. In contrast, weaker host–guest interactions facilitated self-healing. With the same concept, Zhan et al. prepared a gel based on multiple orthogonal interactions [252]. The authors utilized the same interactions as Huang and coworkers [251], but they added another metal–ligand interaction between terpyridine and $Zn(OTf)_2$. The resulting multiresponsive supramolecular gel showed fast self-healing behavior, with broken films showing full recovery after 300 s.

Besides cyclodextrins and crown ethers, cucurbit[*n*]urils (CB[*n*]s) can be utilized to fabricate self-healing materials. CB[*n*]s are cyclic oligomers of glycoluril that can bind single guests such as metals or imidazolium ions ($n = 5$–7). Large guests or even two guests can find space in one CB unit [8] because of the large cavity volume [253]. One example of a healable hydrogel based on CB [8] recognition was published recently by Ikkala and coworkers [254]. The authors synthesized naphthyl-functionalized cellulose nanocrystals and poly(vinyl alcohol) containing methyl viologen to enable host–guest interaction with CB [8] after mixing the compounds together in water. Here, the host acts as dynamic crosslinker

Table 3 Summary of host–guest interactions utilized for self-healing materials

Host	Guest	Literature
Cyclodextrin (CD)		
β-CD	Ferrocene (Fc)	[227, 233–236]
	Adamantane (Ad)	[237–241]
	Azobenzene	[242]
	α-Bromonaphthalene	[243]
	N-Vinylimidazole	[244]
α-CD	*n*-Butane	[237]
Crown ether		
Dibenzo[24]crown-8	Dibenzylammonium	[247–250]
	Cyclohexyl-benzylammonium	[247]
Benzo-21-crown-7	Alkylammonium salt	[251, 252]
Cucurbit[8]urils	Naphthyl/methyl viologen	[254]

of the two different guests. The self-healing properties were investigated with the help of step–strain experiments, demonstrating full recovery of their initial mechanical behavior within a few seconds of damage. Two cut pieces of this hydrogel heal within 30 s. Moreover, calix[*n*]arenes [255, 256] and pillar[*n*]arenes [257, 258] have high potential to be used in self-healing materials because of their cavity size and specific reversible host–guest interactions. Thus, new supramolecular structures should be investigated in order to improve the material properties (i.e. mechanical and self-healing properties) and eventually enable engineering and medical applications [231]. A summary of the host–guest interactions used is given in Table 3.

7 Conclusions and Outlook

Nature itself, as an outstanding demonstrator of self-healing materials, can be a great source of inspiration for the design of novel synthetic smart materials. The interplay of different supramolecular interactions provides the basis for the unique properties of natural materials (systems). Consequently, synthetic supramolecular polymers have been intensively investigated in recent years, because these materials feature interesting properties such as reversibility, stimuli-responsiveness, and tunability of their mechanical properties. Generally, these properties are ideal preconditions for the design of self-healing materials and a variety of different examples have been presented over the last few years.

The properties of these polymers as well as their ability to close cracks can be easily tuned by changing the supramolecular binding motif. Hydrogen bonds feature weak interactions, resulting in rubber-like materials with self-healing properties at room temperature, but metallopolymers reveal much stronger supramolecular bonds. This increase in the binding energy can lead to "stronger" materials,

although external stimuli are often required for such materials to achieve self-healing.

In recent years, a wide range of different systems have been investigated and the underlying healing mechanisms were studied in detail. Nevertheless, there are still many future challenges, such as a complete understanding of the healing mechanism for all supramolecular polymers. Bulk properties and the behavior of the supramolecular unit within the polymer are still poorly understood. The behavior of these moieties and their responsiveness in solution and in the melt are often strongly different; thus, the behavior in bulk still requires other types of investigation. A first study regarding this analysis was performed by Bose et al. [142, 186], who analyzed the behavior of ionomers using rheological measurements. The authors found a crossover of G' and G'' and could correlate this behavior to a supramolecular bond lifetime (τ). This bond lifetime could be used to predict the mechanical and healing properties.

Furthermore, supramolecular systems are also ideal candidates for the commercialization of self-healing materials. Arkema commercialized the polymers investigated by Leibler and coworkers [37], which are similar to the commercially available Surlyn® (http://www.dupont.com/products-and-services/plastics-polymers-resins/ethylene-copolymers/brands/nucrel-ethylene-acrylic-acid.html) or materials from Suprapolix (http://www.suprapolix.com/pages/polymers) which also feature self-healing properties. Nevertheless, more supramolecular systems will appear on the market in the future. Preconditions are the scale-up of the synthesis and, importantly, an improvement in the accessibility of these polymers because many current systems are too expensive for industrial application. Consequently, the basic healing mechanism should be transferred to cheaper systems. Moreover, an intrinsic problem – the creep – of most supramolecular systems has to be solved. The high reversibility of the supramolecular bonds results in a time-dependent response to constant external forces. Introducing additional covalent bonds could remedy this problem but might also reduce the self-healing ability. Alternatively, inclusion of inert rigid particles could lead to a yield point solving the problem without destroying the self-healing characteristics.

The processability of supramolecular self-healing systems also requires more research. Some systems, in particular metallopolymers, were often utilized as networks and synthesized from two compounds, resulting in weakly soluble systems. Thus, the manufacturing of these systems needs to be improved [259–261]. A further challenge is the improvement in the mechanical properties of very good self-healing systems. In general, the supramolecular unit defines the properties of the final polymer. Very weak interactions lead to polymers that are rubber-like, but have a high self-healing capacity. On the other hand, strong supramolecular interactions yield high mechanical properties, but the self-healing ability is reduced and an external stimulus is often required. In recent years, two strategies have been investigated in order to overcome this problem: The first method is to utilize a double network structure with incorporation of covalent crosslinks, which enhance the mechanical properties [56]. Another possibility is a multiphase design in which

both hard and soft segments are utilized to feature both high mechanical properties and self-healing behavior at room temperature [55, 194, 262].

In conclusion, supramolecular systems are well established for the design of self-healing polymers and feature the advantage that their strength is tuneable. Several interactions have been utilized for their preparation, and healing at different temperatures is possible. Thus, an on-demand synthesis of a supramolecular self-healing polymer is possible and the next step towards industrial application is heralded.

Acknowledgements WHB and DD thank the following funding institutions for financial support: funding from the European Union's Seventh Framework Program for research, technological development and demonstration under grant agreement no. 313978 as well as the Deutsche Forschungsgemeinschaft, grant DFG-BI 1337/8–1 and DFG-BI1337/8-2 within the SPP 1568 ("Design and Generic Principles of Self-Healing Materials") and the SFB TRR 102 (project A3).

USS, MDH, ME, and SB thank the Deutsche Forschungsgemeinschaft (DFG, SPP 1568) for financial support.

References

1. Whittell GR, Hager MD, Schubert US, Manners I (2011) Nat Mater 10:176–188
2. Roy D, Cambre JN, Sumerlin BS (2010) Prog Polym Sci 35:278–301
3. Stuart MAC, Huck WTS, Genzer J, Muller M, Ober C, Stamm M, Sukhorukov GB, Szleifer I, Tsukruk VV, Urban M, Winnik F, Zauscher S, Luzinov I, Minko S (2010) Nat Mater 9:101–113
4. Yan X, Wang F, Zheng B, Huang F (2012) Chem Soc Rev 41:6042–6065
5. Lehn J-M (2002) Polym Int 51:825–839
6. Binder W, Zirbs R (2007) Supramolecular polymers and networks with hydrogen bonds in the main- and side-chain. In: Binder WH (ed) Hydrogen bonded polymers, Advances in polymer science. Springer, Berlin, pp 1–78
7. Brunsveld L, Folmer B, Meijer E, Sijbesma R (2001) Chem Rev 101:4071–4098
8. Herbst F, Döhler D, Michael P, Binder WH (2013) Macromol Rapid Commun 34:203–220
9. Michael P, Döhler D, Binder WH (2015) Polymer 69:216–227
10. Green MS, Tobolsky AV (1946) J Chem Phys 14:80–92
11. De Gennes PG (1971) J Chem Phys 55:572–579
12. Leibler L, Rubinstein M, Colby RH (1991) Macromolecules 24:4701–4707
13. Hackelbusch S, Rossow T, van Assenbergh P, Seiffert S (2013) Macromolecules 46:6273–6286
14. Chen X, Dam MA, Ono K, Mal A, Shen H, Nutt SR, Sheran K, Wudl F (2002) Science 295:1698–1702
15. Chen X, Wudl F, Mal AK, Shen H, Nutt SR (2003) Macromolecules 36:1802–1807
16. Kötteritzsch J, Stumpf S, Hoeppener S, Vitz J, Hager MD, Schubert US (2013) Macromol Chem Phys 214:1636–1649
17. de Lucca Freitas L, Stadler R (1988) Colloid Polym Sci 266:1095–1101
18. Stadler R (1993) Kautsch Gummi Kunstst 46:619–628
19. Müller M, Dardin A, Seidel U, Balsamo V, Iván B, Spiess HW, Stadler R (1996) Macromolecules 29:2577–2583
20. Stadler FJ, Pyckhout-Hintzen W, Bailly C (2008) AIP Conf Proc 1027:552–554
21. Subramaniam K, Das A, Simon F, Heinrich G (2013) Eur Polym J 49:345–352

22. Eisenberg A, Hird B, Moore RB (1990) Macromolecules 23:4098–4107
23. Sijbesma RP, Beijer FH, Brunsveld L, Folmer BJB, Hirschberg JHKK, Lange RFM, Lowe JKL, Meijer EW (1997) Science 278:1601–1604
24. Bosman AW, Brunsveld L, Folmer BJB, Sijbesma RP, Meijer EW (2003) Macromol Symp 201:143–154
25. Herbst F, Binder WH (2013) Polym Chem 4:3602–3609
26. Yan T, Schröter K, Herbst F, Binder WH, Thurn-Albrecht T (2014) Macromolecules 47:2122–2130
27. Zare P, Stojanovic A, Herbst F, Akbarzadeh J, Peterlik H, Binder WH (2012) Macromolecules 45:2074–2084
28. Herbst F, Seiffert S, Binder WH (2012) Polym Chem 3:3084–3092
29. Yoon JA, Kamada J, Koynov K, Mohin J, Nicolaÿ R, Zhang Y, Balazs AC, Kowalewski T, Matyjaszewski K (2011) Macromolecules 45:142–149
30. Kolmakov GV, Matyjaszewski K, Balazs AC (2009) ACS Nano 3:885–892
31. Iyer BVS, Salib IG, Yashin VV, Kowalewski T, Matyjaszewski K, Balazs AC (2013) Soft Matter 9:109–121
32. Iyer BVS, Yashin VV, Hamer MJ, Kowalewski T, Matyjaszewski K, Balazs AC (2015) Prog Polym Sci 40:121–137
33. Iyer BVS, Yashin VV, Kowalewski T, Matyjaszewski K, Balazs AC (2013) Polym Chem 4:4927–4939
34. Salib IG, Kolmakov GV, Gnegy CN, Matyjaszewski K, Balazs AC (2011) Langmuir 27:3991–4003
35. Chen Y, Wu W, Himmel T, Wagner MH (2013) Macromol Mater Eng 298:876–887
36. Zhang A, Yang L, Lin Y, Yan L, Lu H, Wang L (2013) J Appl Polym Sci 129:2435–2442
37. Cordier P, Tournilhac F, Soulie-Ziakovic C, Leibler L (2008) Nature 451:977–980
38. Montarnal D, Cordier P, Soulié-Ziakovic C, Tournilhac F, Leibler L (2008) J Polym Sci A Polym Chem 46:7925–7936
39. Montarnal D, Tournilhac F, Hidalgo M, Couturier J-L, Leibler L (2009) J Am Chem Soc 131:7966–7967
40. Tournilhac F, Cordier P, Montarnal D, Soulié-Ziakovic C, Leibler L (2010) Macromol Symp 291–292:84–88
41. Maes F, Montarnal D, Cantournet S, Tournilhac F, Corte L, Leibler L (2012) Soft Matter 8:1681–1687
42. Zhang R, Yan T, Lechner B-D, Schröter K, Liang Y, Li B, Furtado F, Sun P, Saalwächter K (2013) Macromolecules 46:1841–1850
43. Berl V, Schmutz M, Krische MJ, Khoury RG, Lehn J-M (2002) Chem Eur J 8:1227–1244
44. Kolomiets E, Buhler E, Candau SJ, Lehn JM (2006) Macromolecules 39:1173–1181
45. Nair KP, Breedveld V, Weck M (2008) Macromolecules 41:3429–3438
46. Binder WH, Kunz MJ, Ingolic E (2004) J Polym Sci A Polym Chem 42:162–172
47. Binder WH, Kunz MJ, Kluger C, Hayn G, Saf R (2004) Macromolecules 37:1749–1759
48. Kunz MJ, Hayn G, Saf R, Binder WH (2004) J Polym Sci A Polym Chem 42:661–674
49. Binder WH, Bernstorff S, Kluger C, Petraru L, Kunz MJ (2005) Adv Mater 17:2824–2828
50. Binder WH, Machl D (2005) J Polym Sci A Polym Chem 43:188–202
51. Ostas E, Schröter K, Beiner M, Yan T, Thurn-Albrecht T, Binder WH (2011) J Polym Sci A Polym Chem 49:3404–3416
52. Rowan SJ, Suwanmala P, Sivakova S (2003) J Polym Sci A Polym Chem 41:3589–3596
53. Sivakova S, Bohnsack DA, Mackay ME, Suwanmala P, Rowan SJ (2005) J Am Chem Soc 127:18202–18211
54. Hackethal K, Herbst F, Binder WH (2012) J Polym Sci A Polym Chem 50:4494–4506
55. Chen S, Mahmood N, Beiner M, Binder WH (2015) Angew Chem Int Ed 54:10188–10192
56. Döhler D, Peterlik H, Binder WH (2015) Polymer 69:264–273
57. Beijer FH, Kooijman H, Spek AL, Sijbesma RP, Meijer EW (1998) Angew Chem Int Ed 37:75–78

58. Beijer FH, Sijbesma RP, Kooijman H, Spek AL, Meijer EW (1998) J Am Chem Soc 120:6761–6769
59. Kaitz JA, Possanza CM, Song Y, Diesendruck CE, Spiering AJH, Meijer EW, Moore JS (2014) Polym Chem 5:3788–3794
60. Bosman AW, Sijbesma RP, Meijer EW (2004) Mater Today 7:34–39
61. van Gemert GML, Peeters JW, Söntjens SHM, Janssen HM, Bosman AW (2012) Macromol Chem Phys 213:234–242
62. Dankers PYW, Hermans TM, Baughman TW, Kamikawa Y, Kieltyka RE, Bastings MMC, Janssen HM, Sommerdijk NAJM, Larsen A, van Luyn MJA, Bosman AW, Popa ER, Fytas G, Meijer EW (2012) Adv Mater 24:2703–2709
63. Botterhuis NE, van Beek DJM, van Gemert GML, Bosman AW, Sijbesma RP (2008) J Polym Sci A Polym Chem 46:3877–3885
64. Hirschberg JHKK, Beijer FH, van Aert HA, Magusin PCMM, Sijbesma RP, Meijer EW (1999) Macromolecules 32:2696–2705
65. Bobade S, Wang Y, Mays J, Baskaran D (2014) Macromolecules 47:5040–5050
66. Oya N, Ikezaki T, Yoshie N (2013) Polym J 45:955–961
67. Li G, Wie JJ, Nguyen NA, Chung WJ, Kim ET, Char K, Mackay ME, Pyun J (2013) J Polym Sci A Polym Chem 51:3598–3606
68. van Beek DJM, Spiering AJH, Peters GWM, te Nijenhuis K, Sijbesma RP (2007) Macromolecules 40:8464–8475
69. Wietor J-L, van Beek DJM, Peters GW, Mendes E, Sijbesma RP (2011) Macromolecules 44:1211–1219
70. Lewis CL, Stewart K, Anthamatten M (2014) Macromolecules 47:729–740
71. Elkins CL, Park T, McKee MG, Long TE (2005) J Polym Sci A Polym Chem 43:4618–4631
72. Faghihnejad A, Feldman KE, Yu J, Tirrell MV, Israelachvili JN, Hawker CJ, Kramer EJ, Zeng H (2014) Adv Funct Mater 24:2322–2333
73. Feldman KE, Kade MJ, Meijer EW, Hawker CJ, Kramer EJ (2009) Macromolecules 42:9072–9081
74. Folmer BJB, Sijbesma RP, Versteegen RM, van der Rijt JAJ, Meijer EW (2000) Adv Mater 12:874–878
75. Kautz H, van Beek DJM, Sijbesma RP, Meijer EW (2006) Macromolecules 39:4265–4267
76. Keizer HM, van Kessel R, Sijbesma RP, Meijer EW (2003) Polymer 44:5505–5511
77. Sontjens SHM, Renken RAE, van Gemert GML, Engels TAP, Bosman AW, Janssen HM, Govaert LE, Baaijens FPT (2008) Macromolecules 41:5703–5708
78. Fang X, Zhang H, Chen Y, Lin Y, Xu Y, Weng W (2013) Macromolecules 46:6566–6574
79. Kushner AM, Vossler JD, Williams GA, Guan Z (2009) J Am Chem Soc 131:8766–8768
80. Stadler R (1993) Kautsch Gummi Kunstst 46:619–628
81. Peng C-C, Abetz V (2005) Macromolecules 38:5575–5580
82. Chino K, Ashiura M (2001) Macromolecules 34:9201–9204
83. Hilger C, Stadler R (1991) Polymer 32:3244–3249
84. Hilger C, Stadler R, Liane L, Freitas DL (1990) Polymer 31:818–823
85. Müller M, Seidel U, Stadler R (1995) Polymer 36:3143–3150
86. Stadler R, de Lucca Freitas L (1986) Colloid Polym Sci 264:773–778
87. Stadler R, de Araujo MA, Kuhrau M, Rösch J (1989) Makromol Chem 190:1433–1443
88. Schirle M, Hoffmann I, Pieper T, Kilian H-G, Stadler R (1996) Polym Bull 36:95–102
89. Callies X, Fonteneau C, Véchambre C, Pensec S, Chenal JM, Chazeau L, Bouteiller L, Ducouret G, Creton C (2015) Polymer 69:233–240
90. Colombani O, Barioz C, Bouteiller L, Chanéac C, Fompérie L, Lortie F, Montès H (2005) Macromolecules 38:1752–1759
91. Woodward PJ, Hermida Merino D, Greenland BW, Hamley IW, Light Z, Slark AT, Hayes W (2010) Macromolecules 43:2512–2517
92. Ni Y, Becquart F, Chen J, Taha M (2013) Macromolecules 46:1066–1074
93. Roy N, Buhler E, Lehn J-M (2013) Chem Eur J 19:8814–8820

94. Ribagnac P, Cannizzo C, Meallet-Renault R, Clavier G, Audebert P, Pansu RB, Bouteiller L (2013) J Phys Chem B 117:1958–1966
95. Pensec S, Nouvel N, Guilleman A, Creton C, Boué F, Bouteiller L (2010) Macromolecules 43:2529–2534
96. Courtois J, Baroudi I, Nouvel N, Degrandi E, Pensec S, Ducouret G, Chanéac C, Bouteiller L, Creton C (2010) Adv Funct Mater 20:1803–1811
97. Shikata T, Nishida T, Isare B, Linares M, Lazzaroni R, Bouteiller L (2008) J Phys Chem B 112:8459–8465
98. Woodward P, Clarke A, Greenland BW, Hermida Merino D, Yates L, Slark AT, Miravet JF, Hayes W (2009) Soft Matter 5:2000–2010
99. Lortie F, Boileau S, Bouteiller L (2003) Chem Eur J 9:3008–3014
100. Feldman KE, Kade MJ, de Greef TFA, Meijer EW, Kramer EJ, Hawker CJ (2008) Macromolecules 41:4694–4700
101. Feldman KE, Kade MJ, Meijer EW, Hawker CJ, Kramer EJ (2010) Macromolecules 43:5121–5127
102. Ohkawa H, Ligthart GBWL, Sijbesma RP, Meijer EW (2007) Macromolecules 40:1453–1459
103. Ligthart GBWL, Ohkawa H, Sijbesma RP, Meijer EW (2004) J Am Chem Soc 127:810–811
104. Bouteiller L (2007) Assembly via hydrogen bonds of low molar mass compounds into supramolecular polymers. In: Binder W (ed) Hydrogen bonded polymers, vol 207, Advances in polymer science. Springer, Berlin, pp 79–112
105. Knoben W, Besseling NAM, Bouteiller L, Cohen-Stuart MA (2005) Phys Chem Chem Phys 7:2390–2398
106. Lortie F, Boileau S, Bouteiller L, Chassenieux C, Lauprêtre F (2005) Macromolecules 38:5283–5287
107. Lange RFM, Van Gurp M, Meijer EW (1999) J Polym Sci A Polym Chem 37:3657–3670
108. Kuykendall DW, Anderson CA, Zimmerman SC (2008) Org Lett 11:61–64
109. Park T, Todd EM, Nakashima S, Zimmerman SC (2005) J Am Chem Soc 127:18133–18142
110. Park T, Zimmerman SC (2006) J Am Chem Soc 128:13986–13987
111. Park T, Zimmerman SC (2006) J Am Chem Soc 128:11582–11590
112. Park T, Zimmerman SC, Nakashima S (2005) J Am Chem Soc 127:6520–6521
113. Li Y, Park T, Quansah JK, Zimmerman SC (2011) J Am Chem Soc 133:17118–17121
114. Meyer EA, Castellano RK, Diederich F (2003) Angew Chem Int Ed 42:1210–1250
115. Varshey DB, Sander JRG, Friščić T, MacGillivray LR (2012) Supramolecular interactions. In: Steed JW, Gale PA (eds) Supramolecular chemistry. Wiley, Hoboken, pp 9–24
116. Burattini S, Greenland BW, Hayes W, Mackay ME, Rowan SJ, Colquhoun HM (2011) Chem Mater 23:6–8
117. Scott Lokey R, Iverson BL (1995) Nature 375:303–305
118. Greenland BW, Burattini S, Hayes W, Colquhoun HM (2008) Tetrahedron 64:8346–8354
119. Greenland BW, Bird MB, Burattini S, Cramer R, O'Reilly RK, Patterson JP, Hayes W, Cardin CJ, Colquhoun HM (2013) Chem Commun 49:454–456
120. Colquhoun HM, Zhu Z, Williams DJ (2003) Org Lett 5:4353–4356
121. Colquhoun HM, Zhu Z (2004) Angew Chem Int Ed 43:5040–5045
122. Colquhoun HM, Zhu Z, Cardin CJ, Gan Y (2004) Chem Commun 2004(23): 2650–2652
123. Colquhoun HM, Zhu Z, Cardin CJ, Gan Y, Drew MGB (2007) J Am Chem Soc 129:16163–16174
124. Zhu Z, Cardin CJ, Gan Y, Murray CA, White AJP, Williams DJ, Colquhoun HM (2011) J Am Chem Soc 133:19442–19447
125. Burattini S, Colquhoun HM, Greenland BW, Hayes W (2009) Faraday Discuss 143:251–264
126. Burattini S, Colquhoun HM, Fox JD, Friedmann D, Greenland BW, Harris PJF, Hayes W, Mackay ME, Rowan SJ (2009) Chem Commun 2009(44): 6717–6719
127. Burattini S, Greenland BW, Hermida Merino D, Weng W, Seppala J, Colquhoun HM, Hayes W, Mackay ME, Hamley IW, Rowan SJ (2010) J Am Chem Soc 132:12051–12058

128. Hart LR, Hunter JH, Nguyen NA, Harries JL, Greenland BW, Mackay ME, Colquhoun HM, Hayes W (2014) Polym Chem 5:3680–3688
129. Hart LR, Harries JL, Greenland BW, Colquhoun HM, Hayes W (2015) ACS Appl Mater Interfaces 7:8906–8914
130. Hart LR, Nguyen NA, Harries JL, Mackay ME, Colquhoun HM, Hayes W (2015) Polymer 69:293–300
131. Fox J, Wie JJ, Greenland BW, Burattini S, Hayes W, Colquhoun HM, Mackay ME, Rowan SJ (2012) J Am Chem Soc 134:5362–5368
132. Vaiyapuri R, Greenland BW, Rowan SJ, Colquhoun HM, Elliott JM, Hayes W (2012) Macromolecules 45:5567–5574
133. Vaiyapuri R, Greenland BW, Colquhoun HM, Elliott JM, Hayes W (2013) Polym Chem 4:4902–4909
134. Claessens CG, Stoddart JF (1997) J Phys Org Chem 10:254–272
135. Burattini S, Greenland BW, Chappell D, Colquhoun HM, Hayes W (2010) Chem Soc Rev 39:1973–1985
136. Burattini S, Colquhoun HM, Greenland BW, Hayes W (2012) Self-healing and mendable supramolecular polymers. In: Steed JW, Gale PA (eds) Supramolecular chemistry. Wiley, Hoboken, pp 3221–3234
137. Colquhoun HM (2012) Nat Chem 4:435–436
138. Colquhoun H, Klumperman B (2013) Polym Chem 4:4832–4833
139. Hart LR, Harries JL, Greenland BW, Colquhoun HM, Hayes W (2013) Polym Chem 4:4860–4870
140. Vaiyapuri R, Greenland BW, Colquhoun HM, Elliott JM, Hayes W (2014) Polym Int 63:933–942
141. Capek I (2005) Adv Colloid Interf Sci 118:73–112
142. Bose RK, Hohlbein N, Garcia SJ, Schmidt AM, van der Zwaag S (2015) Phys Chem Chem Phys 17:1697–1704
143. James NK, Lafont U, van der Zwaag S, Groen WA (2014) Smart Mater Struct 23:055001
144. Kalista SJ, Pflug JR, Varley RJ (2013) Polym Chem 4:4910–4926
145. Rahman MA, Spagnoli G, Grande AM, Di Landro L (2013) Macromol Mater Eng 298:1350–1364
146. Kalista SJ (2009) Self-healing ionomers. In: Ghosh SK (ed) Self-healing materials: fundamentals, design strategies, and applications. Wiley-VCH, Weinheim, pp 73–100
147. Ma X, Sauer JA, Hara M (1995) Macromolecules 28:3953–3962
148. Tadano K, Hirasawa E, Yamamoto H, Yano S (1989) Macromolecules 22:226–233
149. Eisenberg A (1970) Macromolecules 3:147–154
150. Williams CE, Russell TP, Jerome R, Horrion J (1986) Macromolecules 19:2877–2884
151. Tsujita Y, Hsu SL, MacKnight WJ (1981) Macromolecules 14:1824–1826
152. Squires E, Painter P, Howe S (1987) Macromolecules 20:1740–1744
153. Han K, Williams HL (1991) J Appl Polym Sci 42:1845–1859
154. Zhang L, Brostowitz NR, Cavicchi KA, Weiss RA (2014) Macromol React Eng 8:81–99
155. Hohlbein N, von Tapavicza M, Nellesen A, Schmidt AM (2013) Self-healing ionomers. In: Binder WH (ed) Self-healing polymers: from principles to applications. Wiley-VCH, Weinheim, pp 315–334
156. Varley RJ, van der Zwaag S (2008) Acta Mater 56:5737–5750
157. Pestka KA II, Kalista SJ, Ricci A (2013) AIP Adv 3:082113/082111–082113/082115
158. Bergman SD, Wudl F (2008) J Mater Chem 18:41–62
159. Varley RJ, van der Zwaag S (2008) Polym Test 27:11–19
160. Chen S, Deng Y, Chang X, Barqawi H, Schulz M, Binder WH (2014) Polym Chem 5:2891–2900
161. Malke M, Barqawi H, Binder WH (2014) ACS Macro Lett 3:393–397
162. Fall R (2001) Puncture reversal of ethylene ionomers—mechanistic studies. MSc dissertation. Virginia Polytechnic Institute and State University, Blacksburg

163. Kalista Jr. SJ (2003) Self-healing of thermoplastic poly(ethylene-co-methacrylic acid) copolymers following projectile puncture. MSc dissertation. Virginia Polytechnic Institute and State University, Blacksburg
164. Coughlin CS, Martinelli AA, Boswell RF (2004) Abstr Papers Am Chem Soc 228:261-PMSE. http://oasys2.confex.com/acs/228nm/techprogram/P779385.HTM
165. Kalista SJ Jr, Ward TC, Soc JR (2007) Interface 4:405–411
166. Huber A, Hinkley J (2005) Impression testing of self-healing polymers. NASA technical memorandum, NASA/TM-2005-213532. NASA, Hampton. http://ntrs.nasa.gov/archive/nasa/casi.ntrs.nasa.gov/20050082215.pdf
167. Varley RJ, van der Zwaag S (2010) Polym Int 59:1031–1038
168. Kalista SJ, Ward TC, Oyetunji Z (2007) Mech Adv Mater Struct 14:391–397
169. Haase T, Rohr I, Thoma K (2014) J Intell Mater Syst Struct 25:25–30, 26
170. Varley RJ, Shen S, van der Zwaag S (2010) Polymer 51:679–686
171. Rhaman MA, Penco M, Spagnoli G, Grande AM, Di Landro L (2011) Macromol Mater Eng 296:1119–1127
172. Penco M, Rhaman A, Spagnoli G, Janszen G, Di Landro L (2011) Mater Lett 65:2107–2110
173. Rahman MA, Penco M, Peroni I, Ramorino G, Grande AM, Di Landro L (2011) ACS Appl Mater Interfaces 3:4865–4874
174. Pestka KA, Kalista SJ, Ricci A (2013) AIP Adv 3:082113
175. Grande AM, Castelnovo L, Di Landro L, Giacomuzzo C, Francesconi A, Rahman MA (2013) J Appl Polym Sci 130:1949–1958
176. Francesconi A, Giacomuzzo C, Grande AM, Mudric T, Zaccariotto M, Etemadi E, Di Landro L, Galvanetto U (2013) Adv Space Res 51:930–940
177. Sundaresan VB, Morgan A, Castellucci M (2013) Smart Mater Res 2013:271546
178. Maure S, Furman S, Khor S (2010) Macromol Mater Eng 295:420–424
179. Maure S, Wu DY, Furman S (2009) Acta Mater 57:4312–4320
180. Pingkarawat K, Wang CH, Varley RJ, Mouritz AP (2012) Compos Part A 43:1301–1307
181. Pingkarawat K, Wang CH, Varley RJ, Mouritz AP (2012) J Mater Sci 47:4449–4456
182. Hohlbein N, Shaaban A, Schmidt AM (2015) Polymer 69:301–309
183. Aboudzadeh MA, Munoz ME, Santamaria A, Marcilla R, Mecerreyes D (2012) Macromol Rapid Commun 33:314–318
184. Aboudzadeh MA, Muñoz ME, Santamaría A, Fernández-Berridi MJ, Irusta L, Mecerreyes D (2012) Macromolecules 45:7599–7606
185. Aboudzadeh A, Fernandez M, Munoz ME, Santamaria A, Mecerreyes D (2014) Macromol Rapid Commun 35:460–465
186. Bose RK, Hohlbein N, Garcia SJ, Schmidt AM, van der Zwaag S (2015) Polymer 69:228–232
187. Malmierca MA, González-Jiménez A, Mora-Barrantes I, Posadas P, Rodríguez A, Ibarra L, Nogales A, Saalwächter K, Valentín JL (2014) Macromolecules 47:5655–5667
188. Akbarzadeh J, Puchegger S, Stojanovic A, Kirchner HOK, Binder WH, Bernstorff S, Zioupos P, Peterlik H (2014) Bioinspir Biomime Nanobiomater 3:123–130
189. Sandmann B, Bode S, Hager MD, Schubert US (2013) Adv Polym Sci 262:239–258
190. Holten-Andersen N, Harrington MJ, Birkedal H, Lee BP, Messersmith PB, Lee KYC, Waite JH (2011) Proc Natl Acad Sci USA 108:2651–2655
191. Holten-Andersen N, Jaishankar A, Harrington MJ, Fullenkamp DE, DiMarco G, He L, McKinley GH, Messersmith PB, Lee KYC (2014) J Mater Chem B 2:2467–2472
192. Fullenkamp DE, He L, Barrett DG, Burghardt WR, Messersmith PB (2013) Macromolecules 46:1167–1174
193. Enke M, Bode S, Vitz J, Schacher FH, Harrington MJ, Hager MD, Schubert US (2015) Polymer 69:274–282
194. Mozhdehi D, Ayala S, Cromwell OR, Guan Z (2014) J Am Chem Soc 136:16128–16131
195. Wang Z, Urban MW (2013) Polym Chem 4:4897–4901
196. Yuan J, Fang X, Zhang L, Hong G, Lin Y, Zheng Q, Xu Y, Ruan Y, Weng W, Xia H, Chen G (2012) J Mater Chem 22:11515–11522

197. Hong G, Zhang H, Lin Y, Chen Y, Xu Y, Weng W, Xia H (2013) Macromolecules 46:8649–8656
198. Yang B, Zhang H, Peng H, Xu Y, Wu B, Weng W, Li L (2014) Polym Chem 5:1945–1953
199. Burnworth M, Tang L, Kumpfer JR, Duncan AJ, Beyer FL, Fiore GL, Rowan SJ, Weder C (2011) Nature 472:334–337
200. Martínez-Calvo M, Kotova O, Möbius ME, Bell AP, McCabe T, Boland JJ, Gunnlaugsson T (2015) J Am Chem Soc 137:1983–1992
201. Sandmann B, Happ B, Kupfer S, Schacher FH, Hager MD, Schubert US (2015) Macromol Rapid Commun 36:604–609
202. Terech P, Yan M, Marechal M, Royal G, Galvez J, Velu SKP (2013) Phys Chem Chem Phys 15:7338–7344
203. Bode S, Zedler L, Schacher FH, Dietzek B, Schmitt M, Popp J, Hager MD, Schubert US (2013) Adv Mater 25:1634–1638
204. Kupfer S, Zedler L, Guthmuller J, Bode S, Hager MD, Schubert US, Popp J, Grafe S, Dietzek B (2014) Phys Chem Chem Phys 16:12422–12432
205. Bode S, Bose RK, Matthes S, Ehrhardt M, Seifert A, Schacher FH, Paulus RM, Stumpf S, Sandmann B, Vitz J, Winter A, Hoeppener S, Garcia SJ, Spange S, van der Zwaag S, Hager MD, Schubert US (2013) Polym Chem 4:4966–4973
206. Basak S, Nanda J, Banerjee A (2014) Chem Commun 50:2356–2359
207. Saha S, Bachl J, Kundu T, Diaz Diaz D, Banerjee R (2014) Chem Commun 50:3004–3006
208. Varghese S, Lele A, Mashelkar R (2006) J Polym Sci A Polym Chem 44:666–670
209. Wang Z, Fan W, Tong R, Lu X, Xia H (2014) RSC Adv 4:25486–25493
210. Bode S, Enke M, Bose RK, Schacher FH, Garcia SJ, van der Zwaag S, Hager MD, Schubert US (2015) J Mater Chem A. doi:10.1039/C5TA05545H
211. Hager MD, Greil P, Leyens C, van der Zwaag S, Schubert US (2010) Adv Mater 22:5424–5430
212. Garcia SJ (2014) Eur Polym J 53:118–125
213. Zedler L, Hager MD, Schubert US, Harrington MJ, Schmitt M, Popp J, Dietzek B (2014) Mater Today 17:57–69
214. Harrington MJ, Gupta HS, Fratzl P, Waite JH (2009) J Struct Biol 167:47–54
215. Waite JH, Qin X-X, Coyne KJ (1998) Matrix Biol 17:93–106
216. Waite JH, Vaccaro E, Sun C, Lucas JM (2002) Philos Trans R Soc Lond B 357:143–153
217. Harrington MJ, Waite JH (2007) J Exp Biol 210:4307–4318
218. Harrington MJ, Waite JH (2008) Biomacromolecules 9:1480–1486
219. Harrington MJ, Waite JH (2009) Adv Mater 21:440–444
220. Schmidt S, Reinecke A, Wojcik F, Pussak D, Hartmann L, Harrington MJ (2014) Biomacromolecules 15:1644–1652
221. Harrington MJ, Masic A, Holten-Andersen N, Waite JH, Fratzl P (2010) Science 328:216–220
222. Vaccaro E, Waite JH (2001) Biomacromolecules 2:906–911
223. Degtyar E, Harrington MJ, Politi Y, Fratzl P (2014) Angew Chem Int Ed 53:12026–12044
224. Krogsgaard M, Behrens MA, Pedersen JS, Birkedal H (2013) Biomacromolecules 14:297–301
225. Liu S, Gong W, Yang X (2014) Curr Org Chem 18:2010–2015
226. Houk KN, Leach AG, Kim SP, Zhang X (2003) Angew Chem Int Ed 42:4872–4897
227. Nakahata M, Takashima Y, Yamaguchi H, Harada A (2011) Nat Commun 2:511
228. Saenger W, Steiner T (1998) Acta Cryst A54:798–805
229. Harada A, Takashima Y (2013) Chem Rec 13:420–431
230. Schmidt BVKJ, Hetzer M, Ritter H, Barner-Kowollik C (2014) Prog Polym Sci 39:235–249
231. Yang X, Yu H, Wang L, Tong R, Akram M, Chen Y, Zhai X (2015) Soft Matter 11:1242–1252
232. Moozyckine AU, Bookham JL, Deary ME, Davies DM (2001) J Chem Soc Perkin Trans 2 2001(9):1858–1862

233. Yan Q, Feng A, Zhang H, Yin Y, Yuan J (2013) Polym Chem 4:1216–1220
234. Chuo T-W, Wei T-C, Liu Y-L (2013) J Polym Sci A Polym Chem 51:3395–3403
235. Wang Y-F, Zhang D-L, Zhou T, Zhang H-S, Zhang W-Z, Luo L, Zhang A-M, Li B-J, Zhang S (2014) Polym Chem 5:2922–2927
236. Peng L, Zhang H, Feng A, Huo M, Wang Z, Hu J, Gao W, Yuan J (2015) Polym Chem 6:3652–3659
237. Kakuta T, Takashima Y, Nakahata M, Otsubo M, Yamaguchi H, Harada A (2013) Adv Mater 25:2849–2853
238. Kakuta T, Takashima Y, Sano T, Nakamura T, Kobayashi Y, Yamaguchi H, Harada A (2015) Macromolecules 48:732–738
239. Himmelein S, Lewe V, Stuart MCA, Ravoo BJ (2014) Chem Sci 5:1054–1058
240. Zhang D-L, Ju X, Li L-H, Kang Y, Gong X-L, Li B-J, Zhang S (2015) Chem Commun 51:6377–6380
241. Rodell CB, Wade RJ, Purcell BP, Dusaj NN, Burdick JA (2015) ACS Biomater Sci Eng 1:277–286
242. Dong R, Liu Y, Zhou Y, Yan D, Zhu X (2011) Polym Chem 2:2771–2774
243. Chen H, Ma X, Wu S, Tian H (2014) Angew Chem Int Ed 53:14149–14152
244. Yu C, Wang C-F, Chen S (2014) Adv Funct Mater 24:1235–1242
245. Dong S, Zheng B, Wang F, Huang F (2014) Acc Chem Res 47:1982–1994
246. Pedersen CJ (1967) J Am Chem Soc 89:7017–7036
247. Zhang M, Xu D, Yan X, Chen J, Dong S, Zheng B, Huang F (2012) Angew Chem Int Ed 51:7011–7015, S7011/7011–S7011/7019
248. Zeng F, Han Y, Yan Z-C, Liu C-Y, Chen C-F (2013) Polymer 54:6929–6935
249. Li S, Lu H-Y, Shen Y, Chen C-F (2013) Macromol Chem Phys 214:1596–1601
250. Liu D, Wang D, Wang M, Zheng Y, Koynov K, Auernhammer GK, Butt H-J, Ikeda T (2013) Macromolecules 46:4617–4625
251. Yan X, Xu D, Chen J, Zhang M, Hu B, Yu Y, Huang F (2013) Polym Chem 4:3312–3322
252. Zhan J, Zhang M, Zhou M, Liu B, Chen D, Liu Y, Chen Q, Qiu H, Yin S (2014) Macromol Rapid Commun 35:1424–1429
253. Appel EA, Biedermann F, Rauwald U, Jones ST, Zayed JM, Scherman OA (2010) J Am Chem Soc 132:14251–14260
254. McKee JR, Appel EA, Seitsonen J, Kontturi E, Scherman OA, Ikkala O (2014) Adv Funct Mater 24:2706–2713
255. Guo D-S, Liu Y (2012) Chem Soc Rev 41:5907–5921
256. Yan H, Pan X, Chua MH, Wang X, Song J, Ye Q, Zhou H, Xuan ATY, Liu Y, Xu J (2014) RSC Adv 4:10708–10717
257. Li Z-Y, Zhang Y, Zhang C-W, Chen L-J, Wang C, Tan H, Yu Y, Li X, Yang H-B (2014) J Am Chem Soc 136:8577–8589
258. Ji X, Chen J, Chi X, Huang F (2014) ACS Macro Lett 3:110–113
259. De Gans B-J, Duineveld PC, Schubert US (2004) Adv Mater 16:203–213
260. Janoschka T, Teichler A, Häupler B, Jähnert T, Hager MD, Schubert US (2013) Adv Energy Mater 3:1025–1028
261. Wild A, Teichler A, Ho C-L, Wang X-Z, Zhan H, Schlutter F, Winter A, Hager MD, Wong W-Y, Schubert US (2013) J Mater Chem C 1:1812–1822
262. Chen Y, Kushner AM, Williams GA, Guan Z (2012) Nat Chem 4:467–472